CHAPTER 5

MODEL TESTS ON SINGLE GRANULAR PILE

5.1 General

This chapter mainly discusses two objectives. The primary objective is to determine the optimal mix proportion of the tire chips-aggregate mixture for granular pile applications in soft soils subjected to static and cyclic loading. To achieve this goal, numerous laboratory model tests were performed on ordinary and combi-grid encased granular piles with all five mix proportions of tire chips and aggregates installed in a soft soil bed. The combi-grid was provided as vertical encasement up to the full length. The optimal mix proportion for static loading is analyzed based on load intensity-settlement results, efficiency, and the ultimate load intensity ratio (β). Similarly, for cyclic loading, the optimal mix proportion is analyzed in terms of cyclic-induced settlement of the granular pile (S_c), settlement reduction ratio ($S_{c,r}$), and the development of excess pore water pressure in the surrounding soft soil (P_{exc}).

The second objective is to assess the behavior of a single granular pile under different principal parameters. To achieve this objective, small-scale laboratory model tests were performed on ordinary and encased granular piles composed of the optimum mixture installed in soft soil under static and cyclic loading. The principal parameters considered include different encasement materials and configurations (vertical, horizontal, and combined encasement), cyclic loading amplitudes (q_{cy}) based on the cyclic stress ratio (*CSR*), cyclic loading frequencies (f_{cy}), *L/D* ratios, granular pile end conditions, and surrounding soft soil shear strength (S_u).

5.2 Test series

Four sets of laboratory model tests were conducted on granular piles subjected to static and cyclic loading. The experimental program is outlined in Tables 5.1 to 5.4. Tables 5.1 and 5.2 detail the laboratory model tests on ordinary granular piles (OGP) and vertically encased granular piles with combi-grid encasement (VEGP) up to the full length, aimed at determining the optimal mixture of tire chips and aggregates. Table 5.3 summarizes the laboratory model tests on granular piles composed of the optimal mix proportion using vertical, horizontal, and combined encasements under static loading. The various forms and positions of the combi-grid applied to the granular piles are illustrated in Fig. 5.1. Table 5.4 outlines the laboratory model tests on granular piles under different principal parameters during cyclic loading.

Table 5.1 Summary of model tests on single granular pile with all mix proportions under static loading.

Test no	Test name	D (mm)	L (mm)	GP	A_r (%)	I_D	S_u (kPa)	ET
1	Soil bed	---	---	OS	---	---	8.5	---
2	(0% TC + 100% AG)	60	240	EB	25	70	8.5	None
3	(25% TC + 75% AG)	60	240	EB	25	70	8.5	None
4	(50% TC + 50% AG)	60	240	EB	25	70	8.5	None
5	(75% TC + 25% AG)	60	240	EB	25	70	8.5	None
6	(0% TC + 100% AG)	60	240	EB	25	70	8.5	None
7	(0% TC + 100% AG)	60	240	EB	25	70	8.5	CG
8	(25% TC + 75% AG)	60	240	EB	25	70	8.5	CG
9	(50% TC + 50% AG)	60	240	EB	25	70	8.5	CG
10	(75% TC + 25% AG)	60	240	EB	25	70	8.5	CG
11	(0% TC + 100% AG)	60	240	EB	25	70	8.5	CG

Table 5.2 Summary of model tests on single granular pile with all mix proportions under cyclic loading.

Test no	Test name	D (mm)	L (mm)	GP	A_r (%)	I_D (%)	S_u (kPa)	f_{cy} (Hz)	q_{cy} (kPa)	ET
12	Soil bed	---	---	OS	---	---	8.5	1	85	---
13	(0% TC + 100% AG)	60	240	EB	25	70	8.5	1	85	None
14	(25% TC + 75% AG)	60	240	EB	25	70	8.5	1	85	None
15	(50% TC + 50% AG)	60	240	EB	25	70	8.5	1	85	None
16	(75% TC + 25% AG)	60	240	EB	25	70	8.5	1	85	None
17	(0% TC + 100% AG)	60	240	EB	25	70	8.5	1	85	None
18	(0% TC + 100% AG)	60	240	EB	25	70	8.5	1	85	CG
19	(25% TC + 75% AG)	60	240	EB	25	70	8.5	1	85	CG
20	(50% TC + 50% AG)	60	240	EB	25	70	8.5	1	85	CG
21	(75% TC + 25% AG)	60	240	EB	25	70	8.5	1	85	CG
22	(0% TC + 100% AG)	60	240	EB	25	70	8.5	1	85	CG

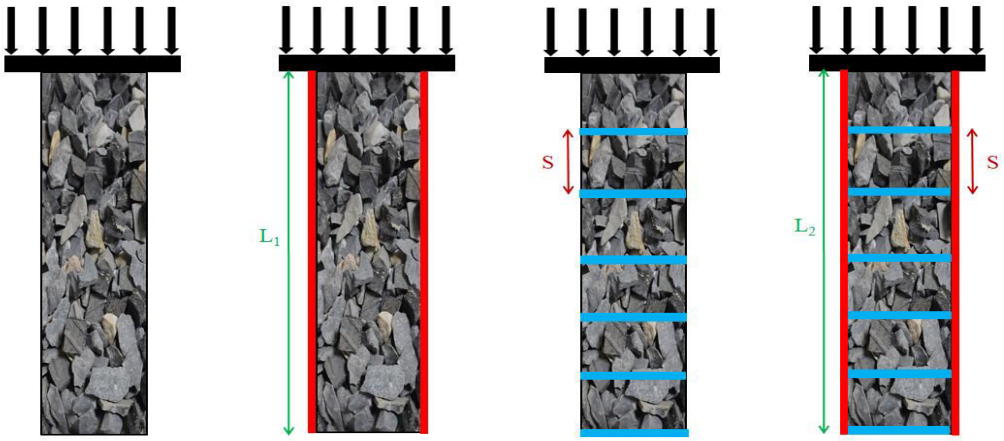

(a) (b) (c) (d)

Fig. 5.1 Schematics of different types of encasements (a) OGP, (b) VEGP, (c) HEGP, and (d) CEGP.

Table 5.3 Summary of model tests on single granular pile with optimum mix proportion under static loading.

Test no	D (mm)	L (mm)	A_r	I_D	S_u (kPa)	GP	ET	L_1	S	L_2
23	60	240	0.25	70	8.5	EB	VEGP	120	---	---
24	60	240	0.25	70	8.5	EB	HEGP	---	15	240
25	60	240	0.25	70	8.5	EB	HEGP	---	15	120
26	60	240	0.25	70	8.5	EB	CEGP	240	15	240
27	60	240	0.25	70	8.5	EB	HEGP	---	30	240
28	60	240	0.25	70	8.5	EB	HEGP	---	30	120
29	60	240	0.25	70	8.5	EB	CEGP	240	30	240
30	60	240	0.25	70	8.5	EB	HEGP	---	60	240
31	60	240	0.25	70	8.5	EB	HEGP	---	60	120
32	60	240	0.25	70	8.5	EB	CEGP	240	60	240

Table 5.4 Summary of single granular pile tests under different principal parameters and cyclic loading.

Series	S_u (kPa)	L/D	ET	f_{cy} (Hz)	q_{cy} (kPa)	N	Type of granular pile
A	8.5	4	GT,GG,CG	1	85	5000	OSB,OGP,VEGP
B	8.5	4	CG	1	85	5000	OGP,VEGP-L,VEGP-0.5L,HEGP-L-0.25D,CEGP-L-0.25D
C	8.5	4	CG	0.5,1,2	85	5000	OSB,OGP,VEGP
D	8.5	4	CG	1	80,85,90	5000	OSB,OGP,VEGP
E	8.5	4,5,6	CG	1	85	5000	OGP,VEGP
F	8.5	4	CG	1	85	5000	EB OGP,EB VEGP, FL OGP,FL VEGP
G	8.5,12.5	4	CG	1	85	5000	OSB,OGP,VEGP

Note: GP = Granular pile; D = Diameter of granular pile; L = Length of granular pile; A_r = Area replacement ratio; I_D = Relative density of granular pile material; S_u = Undrained shear strength of soil bed; f_{cy} = Cyclic loading frequency; q_{cy} = Cyclic loading amplitude; ET = Encasement type; OS = Only soil; EB = End bearing, CG = Combi-grid; VEGP = Vertically encased granular pile; HEGP = Horizontally encased granular pile; CEGP = Combined encased granular pile; L_1 = Length of vertical encasements; L_2 = Length up to which horizontal discs provided; S = Spacing between horizontal discs.

The model tests on single granular piles were studied through the unit cell approach, which assumes the granular pile and surrounding soft soil act as a single unit with a uniform distribution of stresses and strains (Balaam et al. 1977). This

experimental investigation included a total of 60 model tests. The model test set-up is shown in Fig. 5.2. The laboratory model tests performed on the granular piles subjected to static loading were short-term strain-controlled, with loading applied using a load cell at a strain rate of 1 mm/min. Load intensity versus settlement graphs were plotted, and the load intensity at 50 mm settlement was referred to as the ultimate load intensity for comparison. This criterion aligns with the guidelines provided by (Ghazavi and Nazari Afshar 2013; Murugesan and Rajagopal 2007), who also considered settlements up to 50 mm. However, (Ali et al. 2012; Ali et al. 2014) extended the permissible settlement to 60 mm in their studies.

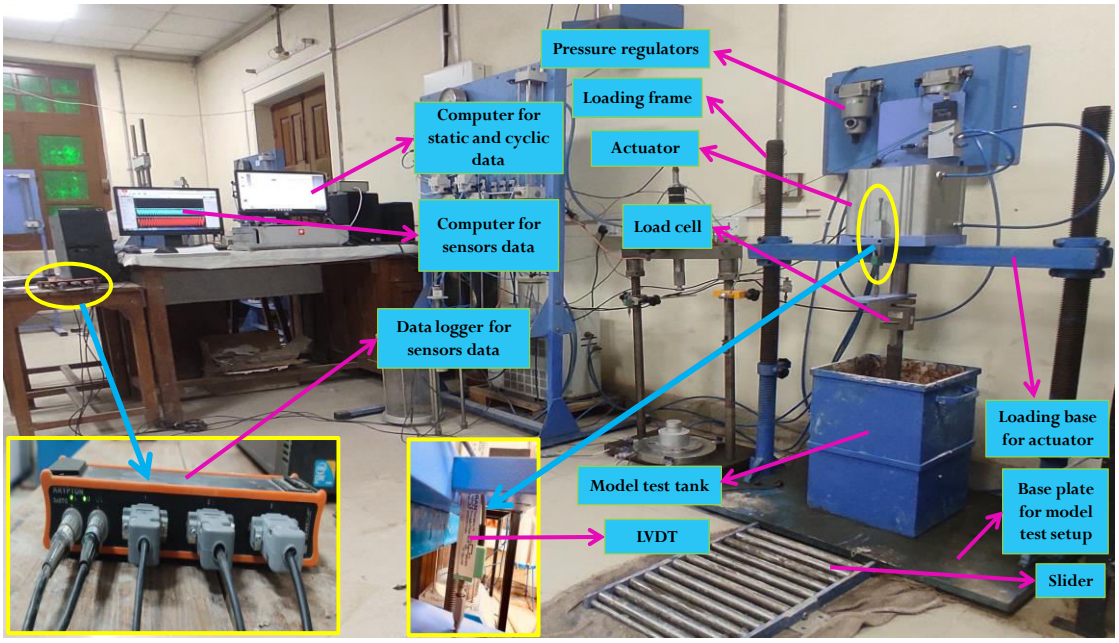

Fig. 5.2 Pictorial representation of model test set-up for single granular pile.

Laboratory model tests were conducted to analyze the cyclic behavior of granular piles. In the case of cyclic loading, stress-controlled tests were performed. In this study, the cyclic loading on granular piles was simulated using a sinusoidal loading wave representing the traffic or train loading, as discussed in 3.3.5. A detailed discussion regarding the testing program and testing parameters considered in both

loading cases was already covered in Chapter 3. The results from the model tests are summarized in the following sections.

5.3 Results and Discussions

5.3.1 Response of granular pile under static loading

5.3.1.1 Analysis of load intensity-settlement behavior of OGP and VEGP

Fig. 5.3 presents the load intensity-settlement behavior of ordinary granular piles (OGP) with various tire chips - aggregates mixtures and notes that the ultimate load intensity gradually changes with different mix proportions. Unreinforced soil (soil bed without granular piles) is also included for comparison purposes. The ultimate bearing capacities of the unreinforced soil bed and OGPs with mix proportions of (0% TC + 100% AG), (25% TC + 75% AG), (50% TC + 50% AG), (75% TC + 25% AG), and (100% TC + 0% AG) are 87.7 kPa, 133.4 kPa, 132.2 kPa, 126.8 kPa, 122 kPa, and 113 kPa, respectively.

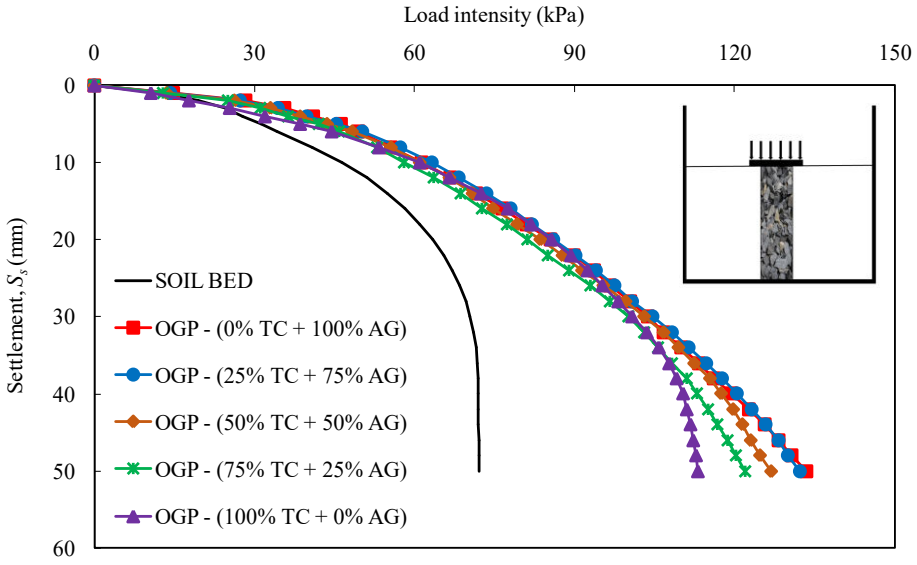

Fig. 5.3 Load intensity-settlement behavior of OGP.

The findings show a gradual reduction in ultimate bearing capacity with increasing tire chip content in the mixture. This trend can be attributed to tire chips lower

stiffness and strength than traditional aggregates. However, with up to 25% tire chip content, there is no reduction in load-bearing capacity. Beyond this, load-bearing capacity is further reduced up to 100% tire chip content. This suggests that a mix containing (25% TC + 75% AG) can provide significant load-bearing capacity, making it a feasible solution for granular piles.

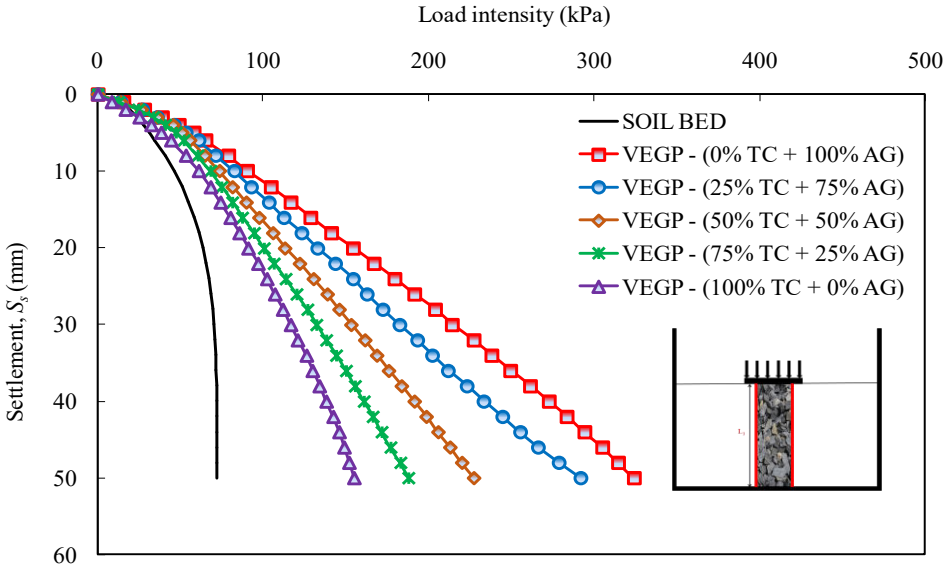

Fig. 5.4 Load intensity-settlement behavior of VEGP ($L_1 = L$).

Similarly, Fig. 5.4 shows the load intensity-settlement behavior of a combi-grid encased granular pile with all mix proportions. The ultimate bearing capacity of the vertically encased granular pile (VEGP) with (0% TC + 100% AG), (25% TC + 75% AG), (50% TC + 50% AG), (75% TC + 25% AG), and (100% TC + 0% AG) are 323.8 kPa, 291.9 kPa, 227.3 kPa, 187.9 kPa, and 155 kPa, respectively. Model tests have demonstrated that the load-carrying capacity of granular piles is substantially improved with full-length combi-grid vertical encasement compared to OGPs. The encasement offers additional lateral support, compensating for the lower stiffness of tire chips and significantly enhancing the performance of the granular pile. Although the ultimate bearing capacity decreases with increasing tire chip content, this trend is

consistent with that observed in ordinary piles. However, the overall capacities remain significantly higher due to the reinforcing effect of the combi-grid.

The study's findings suggest that OGPs with up to 25% tire chips can be effectively used in applications requiring moderate load-bearing capacity. However, combi-grid encased piles present an effective solution for projects requiring higher load capacities. The key finding from the above figures indicates that a combi-grid encased granular pile constructed solely from tire chips (100% TC + 0% AG) exhibits superior load-bearing capacity (=1.16 times) compared to OGP comprised entirely of aggregates (0% TC + 100% AG). Thus, higher bearing capacity was observed with combi-grid encasement even with 100% TC. The test results of OGP and VEGP are presented in Table 5.5.

Table 5.5 Load intensity (kPa) of OGP and VEGP for all mix proportions.

Mix proportion	OGP	VEGP
Soil bed	87.7	87.7
(0% TC + 100% AG)	133.4	323.8
(25% TC + 75% AG)	132.2	291.9
(50% TC + 50% AG)	126.8	227.3
(75% TC + 25% AG)	122	187.9
(100% TC + 0% AG)	113	155

5.3.1.2 Efficiency of optimum mix proportion

Fig. 5.5 shows the variation in the efficiency of OGP and VEGP with all five mix proportions of tire chips and aggregates. (Ayothiraman and Soumya 2015) derived an "efficiency" factor to determine the optimal proportion of tire chips that partially replace aggregates in the granular pile. The "efficiency" factor is defined as the ratio

of the ultimate load intensity of either OGP or VEGP composed of any mix proportion to the ultimate load intensity of OGP composed of 100% aggregates. The granular pile demonstrates maximum performance with OGP composed of 100% aggregates. Therefore, the ultimate load intensity of OGP with (0% TC + 100% AG) was considered 100% efficient and used as a baseline mix proportion for comparison with other mix proportions.

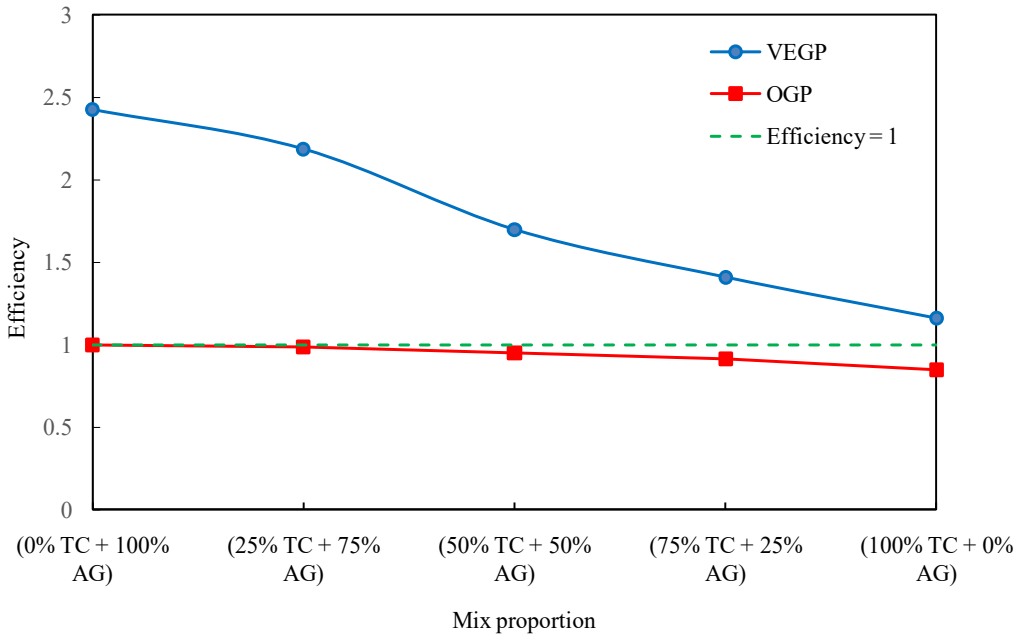

Fig. 5.5 Variation of efficiency of granular pile.

The efficiency of OGP with (25% TC + 75% AG), (50% TC + 50% AG), (75% TC + 25% AG), (100% TC + 0% AG), and only soil bed is 99.1%, 95%, 91.4%, 84.7%, and 65.7%, respectively. The efficiency of the granular pile decreases by 1%, 5%, and 15% for tire chip contents of 25%, 50%, and 100%, respectively. The efficiency of the OGP remains close to 1 up to 25% tire chip content and then progressively decreases with higher tire chip contents. These results suggest that substituting (0% TC + 100% AG) with (25% TC + 75% AG) provides economically and environmentally beneficial outcomes without significantly compromising the

ultimate load intensity of the granular pile. The efficiency loss is less than 1%, while replacing aggregates with waste tire chips offers a positive environmental impact.

The efficiency of VEGP with (0% TC + 100% AG), (25% TC + 75% AG), (50% TC + 50% AG), (75% TC + 25% AG), and (100% TC + 0% AG) is 243.7%, 218.8%, 170.4%, 140.8%, and 116.2%, respectively. The efficiency of VEGP remained above 100% even with 100% tire chip content, highlighting the effectiveness of combi-grid encasement. This suggests that the complete replacement of aggregates with tire chips is feasible when using combi-grid as vertical encasement without compromising the ultimate load intensity.

5.3.1.3 Analysis of load intensity ratio (β)

The ultimate load intensity ratio *(β)* parameter, defined by (Ghazavi and Nazari Afshar 2013; Hasan and Samadhiya 2017), is used to determine the improvement of the soil bed due to the installation of a granular pile.

β is defined as:

$$\beta = \frac{\text{Ultimate load intensity due to granular pile reinforced soil}}{\text{Ultimate load intensity due to only soil bed with no granular pile}} \quad (5.1)$$

The variation of the load intensity ratio (β) with all mix proportions for both OGP and VEGP cases is depicted in Fig. 5.6. From this figure, the β values of OGP with (0% TC + 100% AG), (25% TC + 75% AG), (50% TC + 50% AG), (75% TC + 25% AG), and (100% TC + 0% AG) are 1.52, 1.51, 1.44, 1.39, and 1.29, respectively. It is observed that tire chips have a higher load-carrying capability than the soil bed alone. Similarly, the β values of VEGP with (0% TC + 100% AG), (25% TC + 75% AG), (50% TC + 50% AG), (75% TC + 25% AG), and (100% TC + 0% AG) are 3.69, 3.33, 2.59, 2.14, and 1.77, respectively. Thus, the load-bearing capacity was significantly improved with OGP and increased substantially with combi-grid encasement.

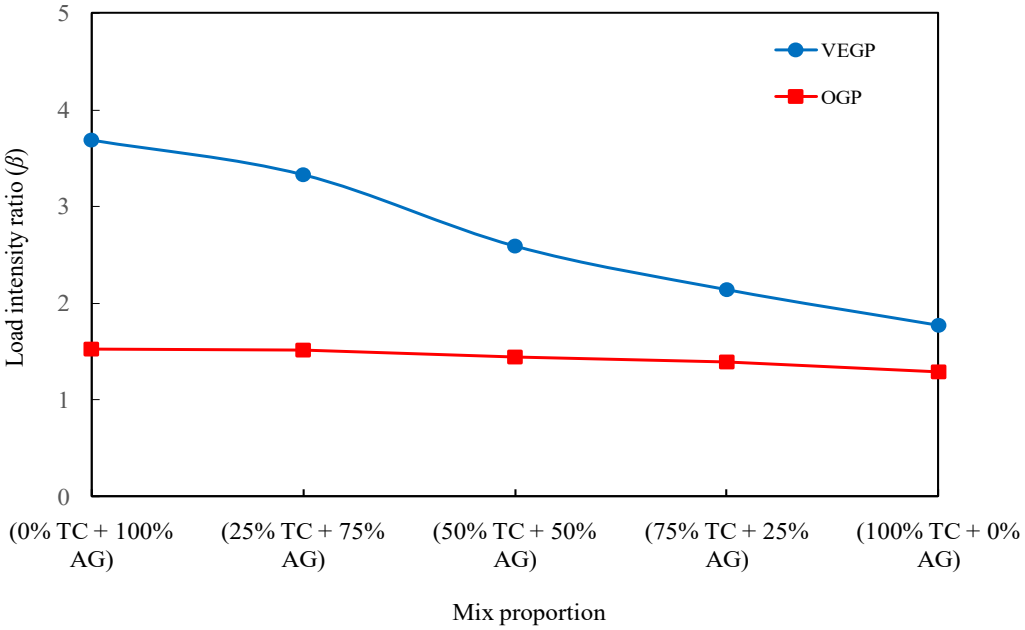

Fig. 5.6 Variation of load intensity ratio (β) with tire chips mixture.

5.3.2 Response of granular pile under cyclic loading

The test parameters considered for the baseline case are combi-grid as the encasement material, a S_u of the soft soil bed of 8.5 kPa, an L/D ratio of 4, and a granular pile end-bearing condition. The cyclic loading parameters considered are a cyclic loading frequency (f_{cy}) of 1 Hz, a cyclic loading amplitude (q_{cy}) of 85 kPa, as per a cyclic stress ratio (CSR) of 0.65, and 5000 cyclic loading cycles, as explained in Section 3.3.5. These parameters remain consistent across all mix proportions. After the model test, the improved soft bed's settlement and excess pore water pressure data were obtained and analyzed.

5.3.2.1 Cyclic induced settlement (S_c) of the loading plate

The accumulated cyclic-induced settlements of the soil bed, OGP, and VEGP for all five mix proportions under cyclic loading are presented in Figs. 5.7(a) and 5.7(b). Each mix proportion within Figs. 5.7(a) and 5.7(b) showcases the cyclic characteristics over the entire 5000-cycle duration.

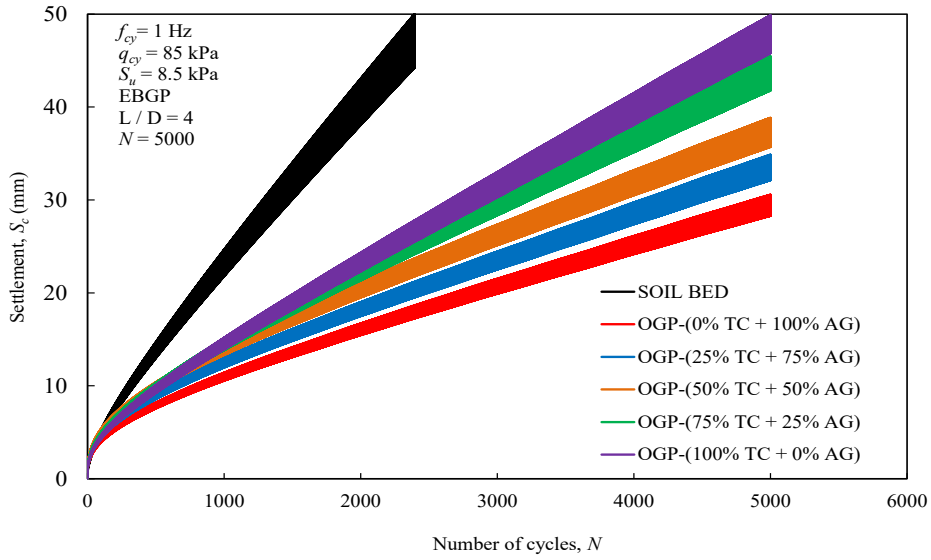

(a)

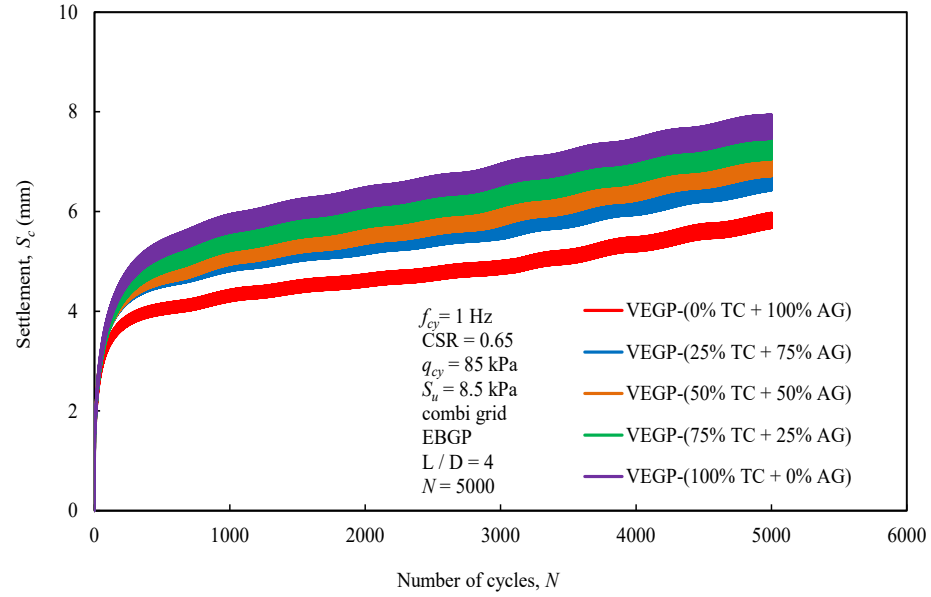

(b)

Fig. 5.7 Cyclic loading responses of five mix proportions with (a) OGP, and (b) VEGP.

In further sections, cyclic-induced settlement (S_c) curves were plotted by considering all the peak points at intervals of 100 cycles up to 5000 cycles. Similar curves were plotted by (Yoo and Abbas 2020; Zhang et al. 2020; Yuan et al. 2021; Gao et al. 2021; Ashour et al. 2022; Cui et al. 2023; Shahu et al. 2023). The peak

cyclic-induced settlements of the soil bed, OGP, and VEGP for all five mix proportions under cyclic loading are presented in Figs. 5.8(a-c).

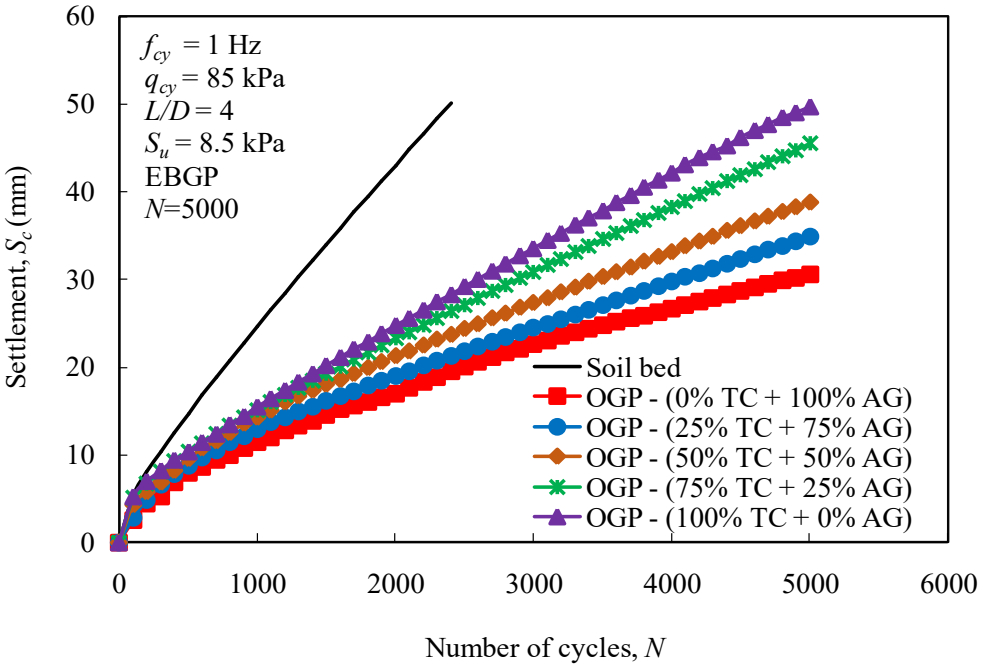

(a)

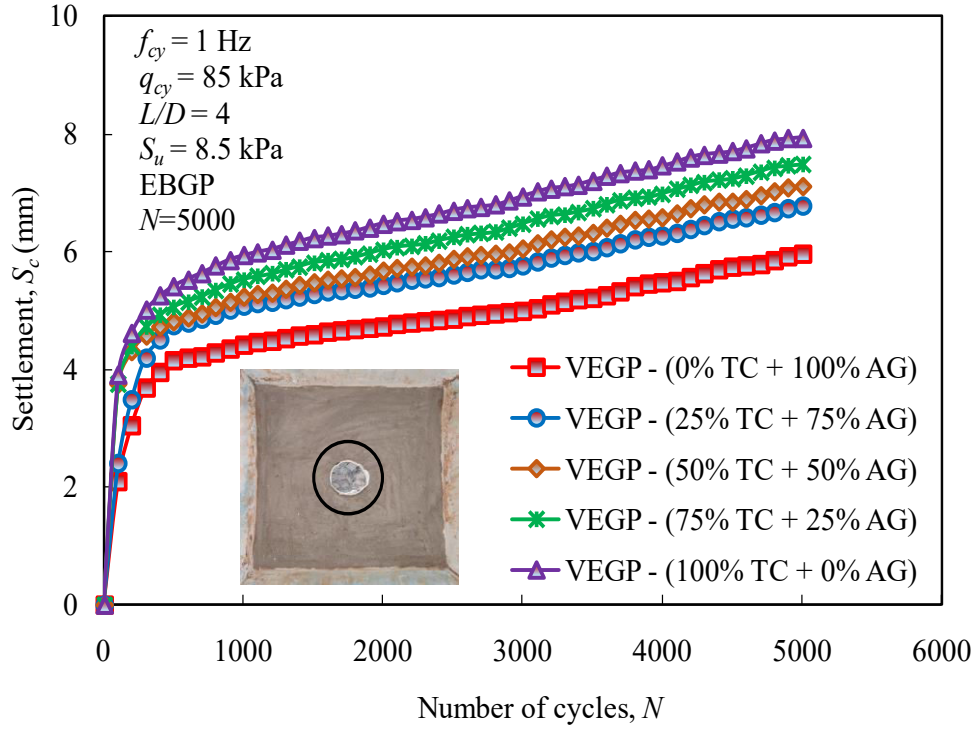

(b)

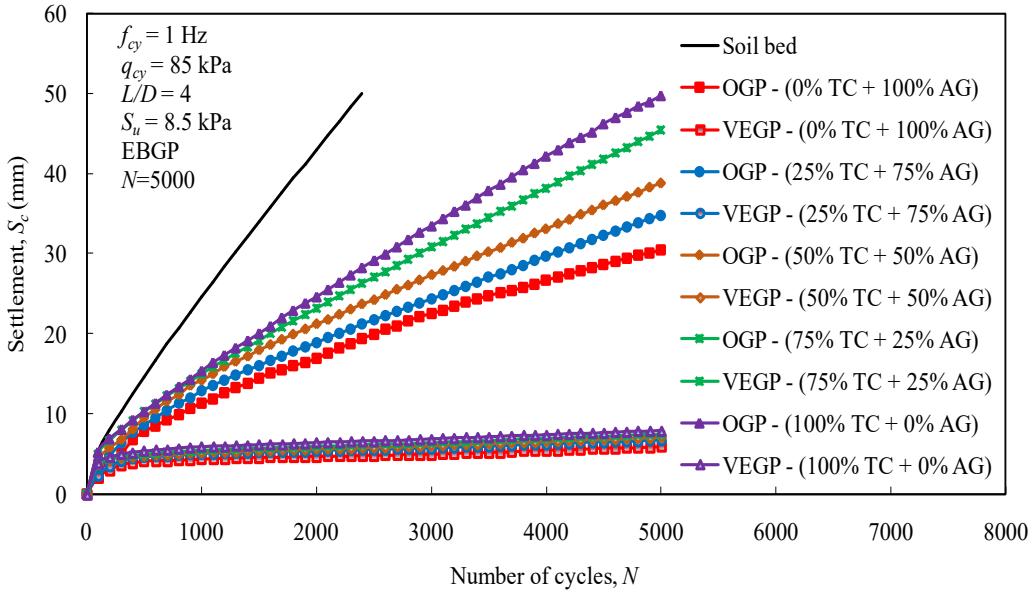

(c)

Fig. 5.8 Cyclic loading responses of five mix proportions with (a) OGP, (b) VEGP, and, (c) both.

From Figs. 5.8(a) and 5.8(b), it can be observed that in the case of a soil bed without any granular pile, the accumulated settlement develops very rapidly and reaches the maximum limit of 50 mm within 2500 load cycles. Similarly, in the case of OGP, the accumulated settlement develops rapidly up to 5000 load cycles for all mix proportions. However, in the case of VEGP, the progression of accumulated settlement undergoes rapid development during the initial 500 loading cycles, followed by gradual stabilization. The peak accumulated settlements of both OGP and VEGP are shown in Fig. 5.8(c).

Due to equipment limitations, the maximum cyclic-induced settlement of granular piles considered in this study is 50 mm, consistent with the static case. The maximum settlement values of the soil bed, OGP with (0% TC + 100% AG), (25% TC + 75% AG), (50% TC + 50% AG), (75% TC + 25% AG), and (100% TC + 0% AG) are 50 mm within 2500 load cycles, 30.6 mm, 34.8 mm, 38.8 mm, 45.5 mm, and 50 mm,

respectively. Similarly, the settlement values of VEGP with (0% TC + 100% AG), (25% TC + 75% AG), (50% TC + 50% AG), (75% TC + 25% AG), and (100% TC + 0% AG) are 6 mm, 6.8 mm, 7.1 mm, 7.5 mm, and 8 mm, respectively. Model test results reveal that the cyclic-induced settlement of the soft soil bed is significantly reduced with the installation of OGP and substantially reduced with the VEGP.

The model test results demonstrate the effectiveness of using granular piles, both with and without combi-grid encasement, in reducing the cyclic-induced settlement of soft soil beds. The OGP configurations show a progressive increase in settlement as the tire chip (TC) content increases, with the settlement values approaching the maximum of 50 mm at higher TC contents. In contrast, the VEGP configurations exhibit substantially lower settlement values across all mix proportions, indicating superior performance in mitigating cyclic-induced settlements.

5.3.2.2 Efficiency of optimum mix proportion

In the case of static loading, the optimum mix proportion of the tire chips - aggregates mixture was selected based on the "efficiency" factor. The efficiency factor is defined as the ratio of the ultimate load intensity of either OGP or VEGP composed of any mix proportion to the ultimate load intensity of OGP composed of 100% aggregates. However, in the case of cyclic loading, the efficiency factor is defined in terms of cyclic-induced settlement (S_c), which is the ratio of S_c of OGP composed of 100% aggregates to the Sc of either OGP or VEGP composed of any mix proportion.

The granular pile demonstrates optimal performance with OGP comprising 100% aggregates. Therefore, the cyclic-induced settlement of OGP with (0% TC + 100% AG) was regarded as 100% efficient and compared against other mix proportions, similar to the static case. Fig. 5.9 represents the efficiency variation of OGP and VEGP for all five mix proportions. The efficiency of OGP with (25% TC + 75% AG),

(50% TC + 50% AG), (75% TC + 25% AG), and (100% TC + 0% AG) is 87.6%, 78.7%, 67.2%, and 61.4%, respectively. The percentage decrease in efficiency is nearly 12%, 21%, 33%, and 39% for tire chip contents of 25%, 50%, 75%, and 100%, respectively. The efficiency loss with 25% tire chip content is merely 12%, a notably smaller reduction. However, this substitution of aggregates with recycled tire chips contributes positively to sustainable infrastructure development.

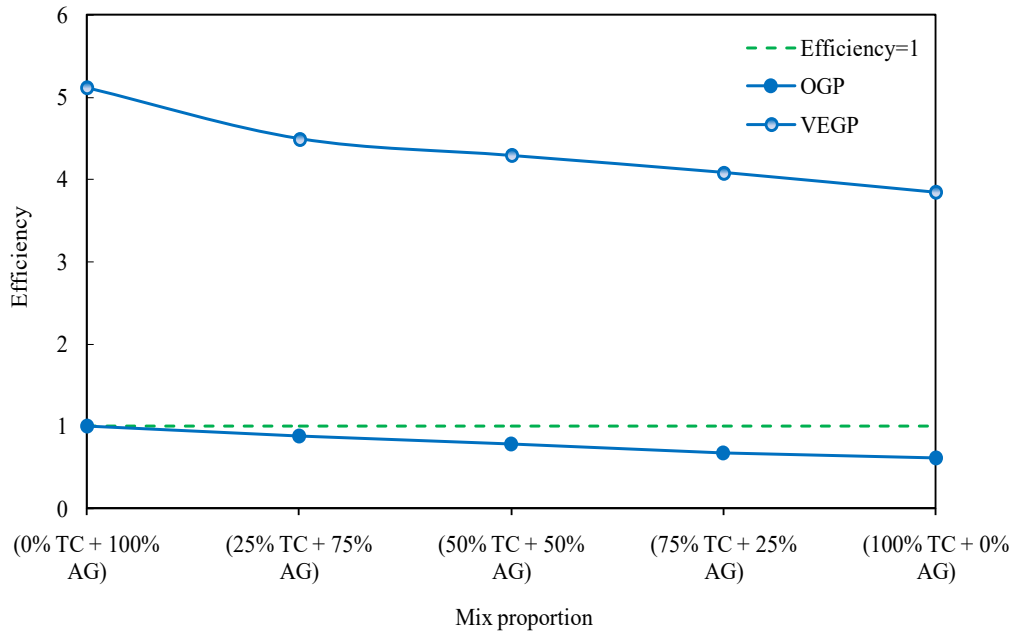

Fig. 5.9 Efficiency variation of five mix proportions with (0% TC + 100% AG).

The granular pile demonstrates optimal performance with OGP comprising 100% aggregates. Therefore, the cyclic-induced settlement of OGP with (0% TC + 100% AG) was regarded as 100% efficient and compared against other mix proportions, similar to the static case. Fig. 5.9 represents the efficiency variation of OGP and VEGP for all five mix proportions. The efficiency of OGP with (25% TC + 75% AG), (50% TC + 50% AG), (75% TC + 25% AG), and (100% TC + 0% AG) is 87.6%, 78.7%, 67.2%, and 61.4%, respectively. The percentage decrease in efficiency is nearly 12%, 21%, 33%, and 39% for tire chip contents of 25%, 50%, 75%, and 100%,

respectively. The efficiency loss with 25% tire chip content is merely 12%, a notably smaller reduction. However, this substitution of aggregates with recycled tire chips contributes positively to sustainable infrastructure development.

The impact of combi-grid encasement on the granular pile is also described using the settlement reduction ratio ($S_{c,r}$), as reported by (Yoo and Abbas 2019; Gao et al. 2021), which is defined as

$$S_{c,r} = \frac{S_{EGP}}{S_{OGP}} \tag{5.2}$$

where $S_{c,r}$ is the settlement reduction ratio, S_{EGP} is the settlement of encased granular pile (in this study, EGP = VEGP), and S_{OGP} is the settlement of ordinary granular pile. Fig. 5.10presents the $S_{c,r}$ values as 0.20, 0.21, 0.23, 0.25, and 0.26 for granular piles with tire contents of 0%, 25%, 50%, 75%, and 100%, respectively. This demonstrates that VEGP reduced the cyclic-induced settlement of the granular pile by approximately 80%, 79%, 77%, 75%, and 74% compared to OGP for tire contents of 0%, 25%, 50%, 75%, and 100%, under cyclic loading, respectively. This highlights the significant reduction in cyclic-induced settlement of the granular pile achieved by combi-grid encasement, irrespective of the mix proportion.

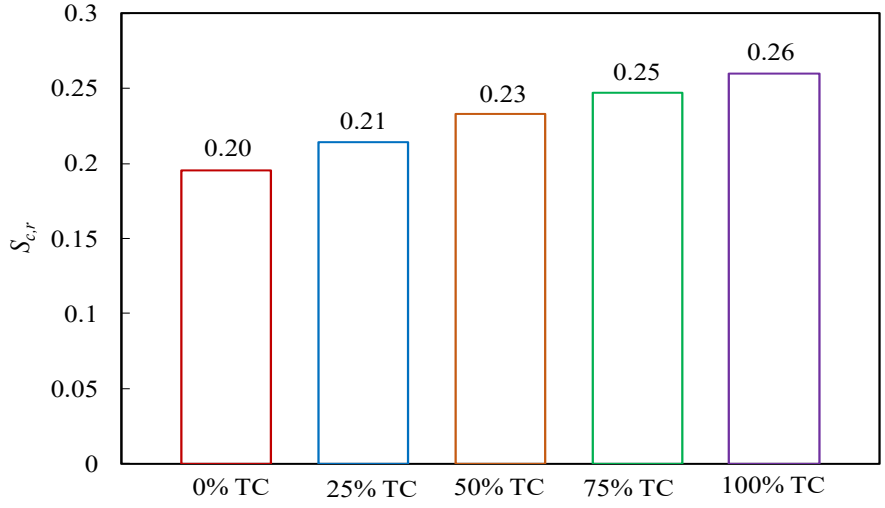

Fig. 5.10 Settlement reduction ($S_{c,r}$) ratios of five mix proportions with tire content.

5.3.2.3 Accumulation of excess pore water pressure (P_{exc}) in the surrounding soil

The settlement behavior of a granular pile-improved soft soil bed is intimately associated with the generation of excess pore water pressure (P_{exc}) resulting from cyclic loading. The pore water pressure has significant effects on the geotechnical behavior of soils. The accumulation of excess pore water pressure (P_{exc}) results in a reduction of the effective stress within the soil bed, thereby decreasing the bearing capacity of the composite ground and potentially inducing liquefaction in silty soils with considerable sand percentages (Polito et al. 2008). The mitigation of excess pore water pressure is necessary to improve the ground's engineering properties. Hence, it is vital to thoroughly assess and effectively manage excess pore water pressure in geotechnical engineering projects. Granular piles are well-suited for reducing P_{exc} from the surrounding soil by providing an efficient drainage path.

The P_{exc} was monitored using a pore pressure transducer installed in the middle of the soil bed (150 mm below the loading plate) at 60 mm from the pile center. The P_{exc} in the surrounding soil for the soil bed, OGP, and VEGP, for all five mix proportions under cyclic loading, is presented in Figs. 5.11 and 5.12.

Fig. 5.11 represents the cyclic characteristics of P_{exc} variations over the entire 5000-cycle duration. The cumulative excess pore water pressure (P_{exc}) curves were plotted by considering all the peak points at intervals of 100 cycles, up to 5000 cycles, similar to the cyclic-induced settlement graphs. The maximum P_{exc} variations of the soil bed, OGP, and VEGP for all five mix proportions under cyclic loading are presented in Fig. 5.12. From these figures, it is observed that P_{exc} increases very rapidly in the soil bed. However, for both OGP and VEGP, the accumulation of pore water pressure experiences rapid development during the initial 2000 loading cycles,

followed by a gradual stabilization. The peak values of P_{exc} are considered concerning a maximum cyclic-induced settlement value of 50 mm.

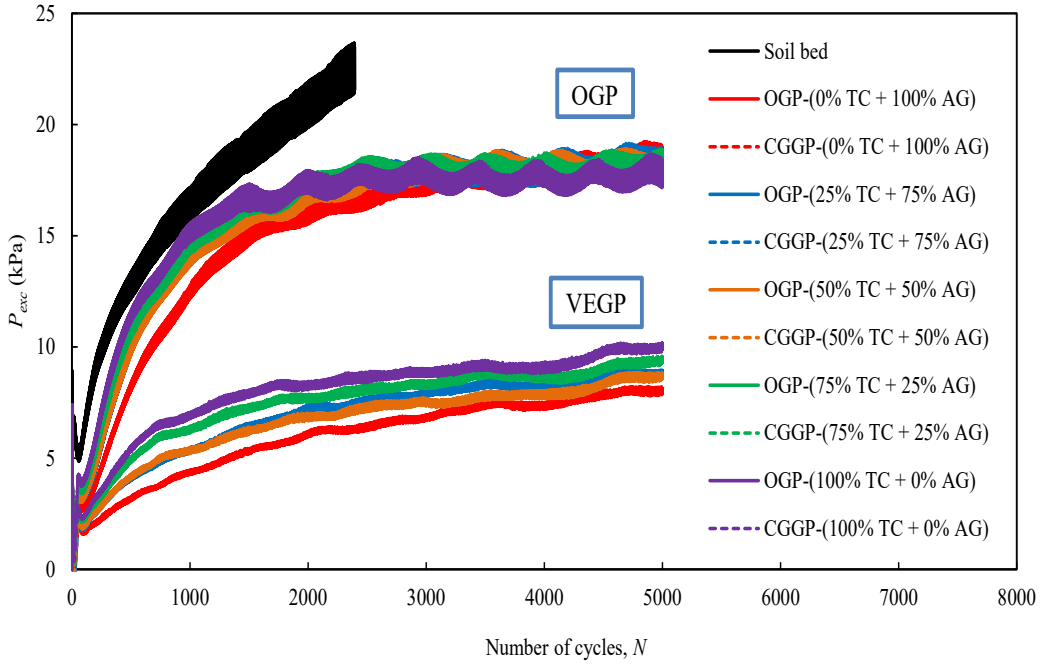

Fig. 5.11 Excess pore water (P_{exc}) responses of five mix proportions for soil bed, OGP, and VEGP.

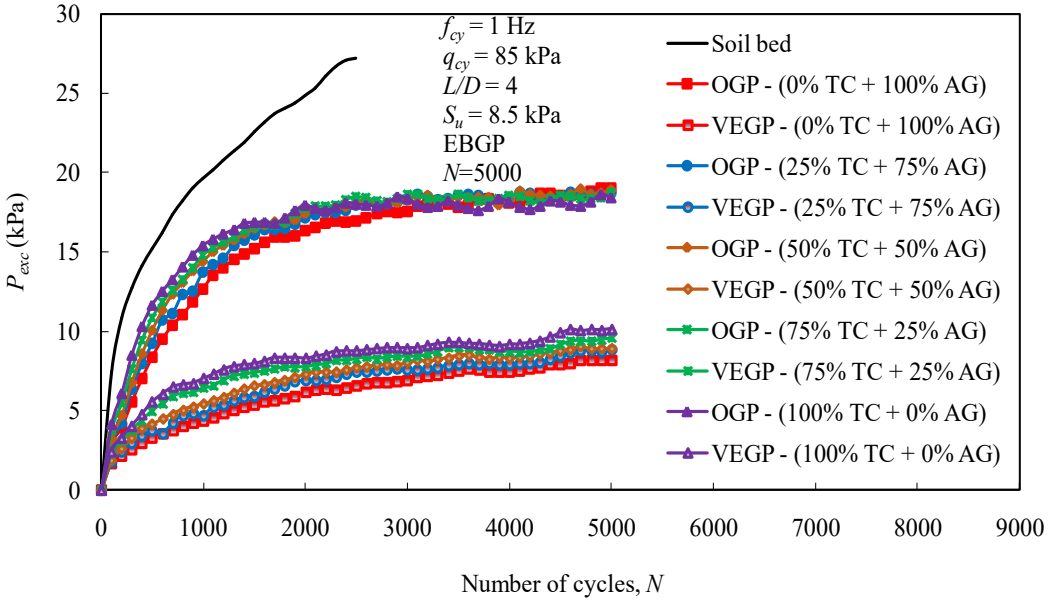

Fig. 5.12 Peak excess pore water (P_{exc}) responses of five mix proportions for soil bed, OGP, and VEGP.

The peak P_{exc} values of the soil bed, OGP with (0% TC + 100% AG), (25% TC + 75% AG), (50% TC + 50% AG), (75% TC + 25% AG), and (100% TC + 0% AG) are 27.2 kPa within 2500 load cycles, 18.7 kPa, 18.7 kPa, 18.7 kPa, 18.8 kPa, and 18.8 kPa, respectively, demonstrating that the peak values of P_{exc} are approximately the same for all five mix proportions. Similarly, the peak P_{exc} values of VEGP with (0% TC + 100% AG), (25% TC + 75% AG), (50% TC + 50% AG), (75% TC + 25% AG), and (100% TC + 0% AG) are 8.16 kPa, 8.9 kPa, 9.2 kPa, 9.6 kPa, and 10.1 kPa, respectively. The model test results illustrate that the P_{exc} of the soft soil bed experiences a notable reduction with the installation of OGP, irrespective of mix proportion, and undergoes a significant decrease with the provision of vertical combi-grid encasement for full length. Additionally, the VEGP exclusively built from (100% TC + 0% AG) showcases a significant decrease in accumulated excess pore water pressure within the surrounding soil bed, approximately 1.85 times greater than that of an OGP composed of (0% TC + 100% AG). Hence, even with a composition of 100% tire chips, the combi-grid encasement demonstrates a superior decrease in P_{exc}.

From the preceding discussions, and similar to Chapter 4, a granular pile (25% TC + 75% AG) is considered the optimal mix proportion. This mix does not compromise load-bearing capacity, effectively reduces cyclic-induced settlement and excess pore water pressure accumulation in the surrounding soft bed, and offers an environmentally friendly solution. Therefore, a granular pile (25% TC + 75% AG) is selected for further analysis.

5.3.3 Response of different configurations of encasements under static loading

The laboratory model tests related to different forms of combi-grid encasement to granular piles under static loading are illustrated in Table 5.3.Fig. 5.1 presents a schematic illustration of the provision of encasement in different configurations to

granular piles. The laboratory results of end-bearing granular piles encased with full and half-length horizontal discs at three different spacings are illustrated in Fig. 5.13(a) and Fig. 5.13(b).

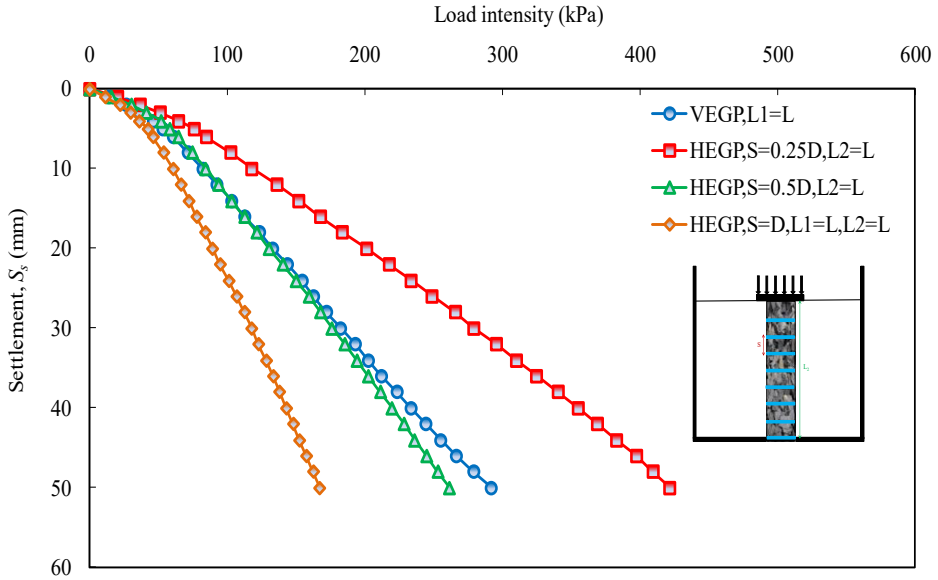

(a)

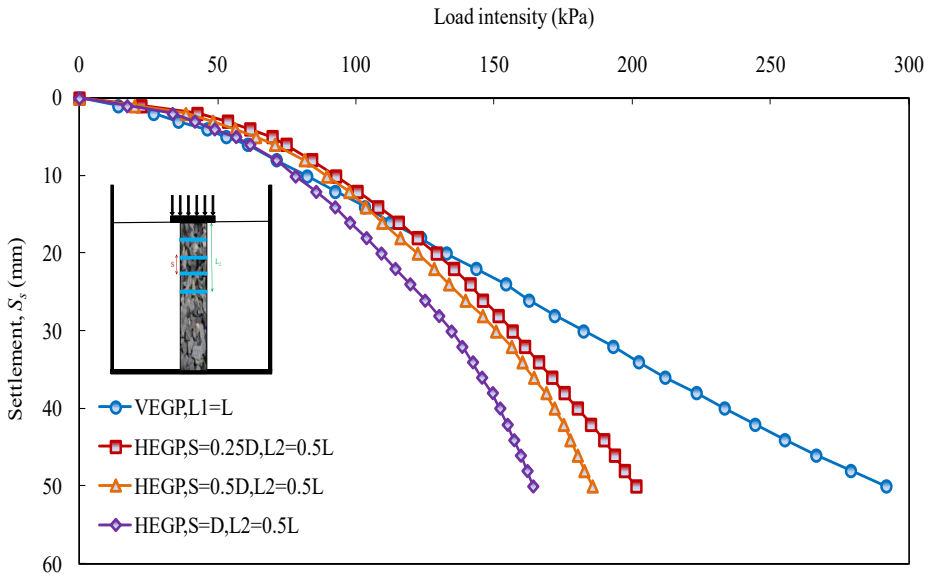

(b)

Fig. 5.13 Variation of load intensity-settlement of granular piles with horizontal discs (a) Full vertical length ($L_2 = L$),and (b) Half vertical length ($L_2 = 0.5L$).

Fig. 5.13(a) shows the provision of combi-grid encasement in horizontal discs for the full length with spacings of 0.25D, 0.5D, and D and compares these results with VEGP with full encasement. Model tests have shown that the ultimate load intensity of granular piles improves with the decrease in the spacing of horizontal discs, and the test results are presented in Table 5.6.

The ultimate load intensities of HEGP with 0.25D, 0.5D, and D spacing are 421.5 kPa, 261.4 kPa, and 167.04 kPa, respectively. The ultimate bearing capacities of HEGP with 0.25D, 0.5D, and D spacing increased by 218.8%, 97.7%, and 26.3% compared to OGP with (25% TC + 75% AG). The percentage increment from HEGP with 0.25D to VEGP with (25% TC + 75% AG) is 44.4%, while the percentage decrement from HEGP with 0.5D and D to VEGP is 10.5% and 42.3%, respectively. The ultimate bearing capacity of HEGP with 0.25D spacing is 1.44 times that of VEGP with full encasement. The improvement in ultimate bearing capacity is due to the mobilization of frictional resistance between the horizontal discs and the granular pile material.

Similarly, Fig. 5.13(b) shows the provision of encasement in the form of horizontal discs for half-length with spacings of 0.25D, 0.5D, and D and compares these results with encased granular piles with VEGP, showing a similar trend as the full length. The test results are presented in Table 5.6. The ultimate load intensities of HEGP with 0.25D, 0.5D, and D spacing are 201.3 kPa, 181.5 kPa, and 164.1 kPa, respectively. The ultimate load intensities of HEGP for 0.25D, 0.5D, and D spacing increased by 52.2%, 37.3%, and 24.1% compared to OGP with (25% TC + 75% AG) and decreased by 31%, 37.8%, and 43.8% compared to VEGP with (25% TC + 75% AG), respectively.

In addition, experiments were conducted to investigate the combined effect of vertical encasement and horizontal discs for granular piles composed of (25% TC + 75% AG). Limited research has been carried out on combined encasement. Fig. 5.14 illustrates the provision of encasement in the combined form for full length with spacings of 0.25D, 0.5D, and D. The ultimate load intensities of CEGP with 0.25D, 0.5D, and D spacing for full-length encasement are 513.5 kPa, 371.2 kPa, and 293.2 kPa, respectively. The ultimate load intensities of CEGP for 0.25D, 0.5D, and D spacing increased by 288.4%, 180.8%, and 121.8% compared to OGP with (25% TC + 75% AG), and by 75.9%, 27.2%, and 0.4% compared to VEGP with (25% TC + 75% AG), respectively. The ultimate load intensity of CEGP with 0.25D spacing was 1.76 times that of VEGP with full encasement and 1.22 times that of HEGP with 0.25D spacing up to the full length. The ultimate bearing capacity of granular piles is further enhanced due to mobilizing hoop stresses and frictional resistance between the combi-grid encasement and granular pile material.

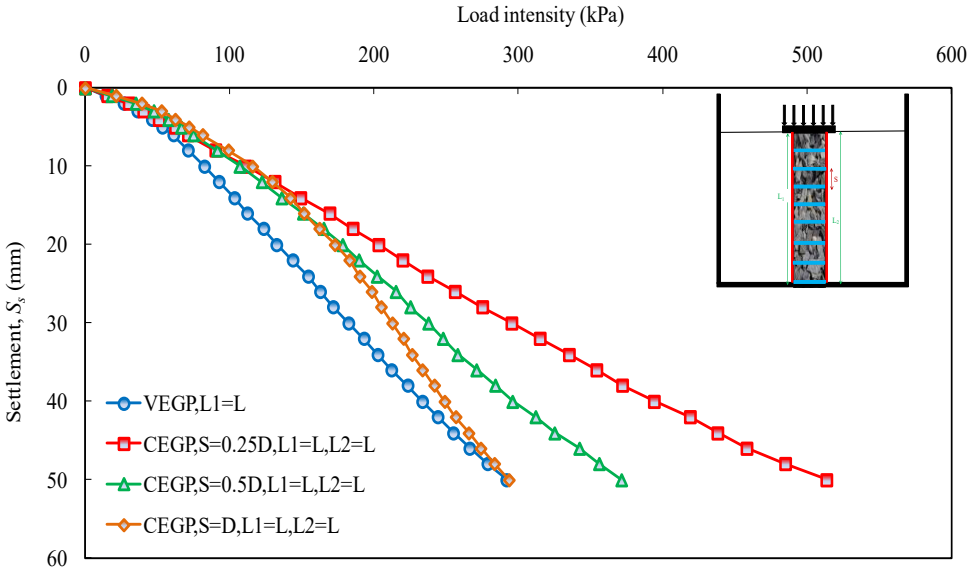

Fig. 5.14 Variation of load intensity settlement behavior of granular piles with combined vertical encasement and horizontal discs ($L_1 = L$, $L_2 = L$).

Table 5.6 Load intensity (kPa) and load intensity ratio(β) of vertical, horizontal and combined encasement.

Encasement type	L_1 (mm)	S (mm)	L_2 (mm)	q_{us}(kPa)	β
VEGP	240	---	---	291.9	3.33
VEGP	120	---	---	164.1	1.87
HEGP	---	0.25D	240	421.5	4.81
HEGP	---	0.25D	120	201.3	2.29
CEGP	240	0.25D	240	513.5	5.85
HEGP	---	0.5D	240	261.4	2.98
HEGP	---	0.5D	120	185.5	2.11
CEGP	240	0.5D	240	371.2	4.23
HEGP	---	D	240	167.0	1.90
HEGP	---	D	120	164.1	1.87
CEGP	240	D	240	293.2	3.34

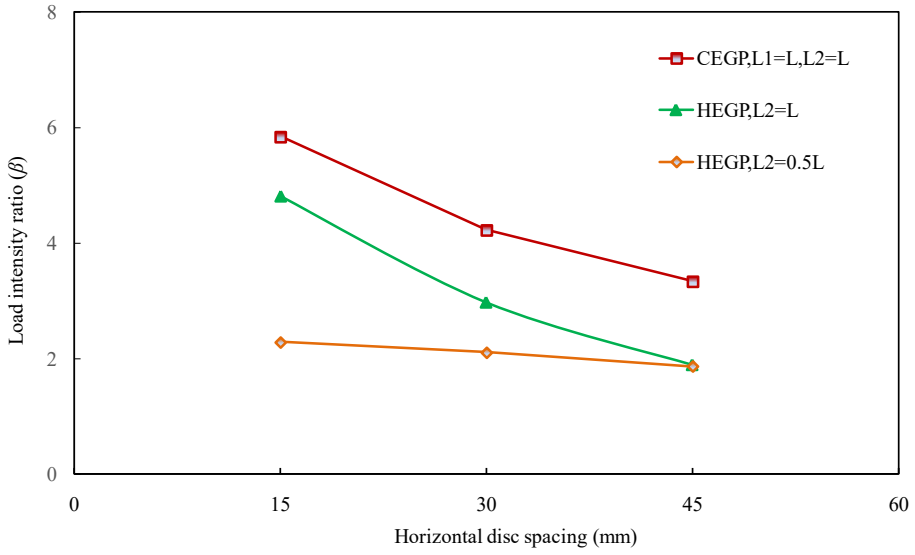

Fig. 5.15 Variation of load intensity ratio (β) with horizontal discs and combined encasement.

The variation of the load intensity ratio (β) of the optimum mixture (25% TC + 75% AG) with HEGP and VEGP with three spacings is depicted in Fig. 5.15. From the figure, the β values of HEGP for 0.25D, 0.5D, and D spacing for full length are

4.81, 2.98, and 1.90, respectively; for half-length, they are 2.29, 2.11, and 1.87, respectively. Similarly, the β values of CEGP for 0.25D, 0.5D, and D spacing are 5.85, 4.23, and 3.34, respectively. The range of β values from experimental results is presented in Table 5.6.

5.3.3.1 The influence of tire content on granular pile bulging behavior

Fig. 5.16 Typical lateral deformation/bulging of (25% TC + 75% AG) (a) OGP, (b) VEGP,(c) HEGP-0.25D,and (d) CEGP-0.25D.

After the testing, plaster of Paris was utilized to develop the bulging patterns of the granular piles. These patterns were observed for various granular piles, including OGP, VEGP, HEGP with 0.25D spacing, and CEGP with 0.25D spacing, all composed of the optimum mixture (25% TC + 75% AG). These bulging patterns are represented in Fig. 5.16, providing visual insights into the lateral deformations resulting from the experimental studies. This visual analysis complements the quantitative data obtained from the experiments, enhancing the understanding of the performance of different pile configurations.

5.3.4 Effect of principle parameters on the behavior of granular piles under cyclic loading

The relationship between train speed and loading frequency at the sub-grade level was calculated using a formula proposed by (Ashour et al. 2022), as explained in Chapter 3.3.5.

$$f = \frac{V}{3.6L} \tag{5.3}$$

where f is the frequency of subgrade displacement (Hz), V is the train speed (km/hr), and L is the length of the train coach (m). The average speed of trains in India ranges from 36 km/hr to 113 km/hr, as per the Ministry of Railways, Government of India. The average speed considered in this study is 90 km/hr. The average length of a railway coach in India is 25 m. By considering these values, the loading frequency is calculated as 1 Hz. The other loading frequencies considered are 0.5 Hz and 2 Hz, representing a train speed of 50 km/hr and 180 km/hr.

The relationship between train speed, axle load, and cyclic loading amplitude at the sub-grade level was calculated using a proposed formula (Cai et al. 2020;Ashour et al. 2022).

$$\sigma_d = 0.26P + 0.26P\alpha V \tag{5.4}$$

where σ_d is the dynamic vertical stress on the subgrade (kPa), P is the train axle load (kN), V is the train speed (km/hr), and α is the speed coefficient and is considered 0.005 for high-speed railways. The axle load of Vande Bharat Express in India is 170 kN, and three train speeds of 160 km/hr, 180 km/hr, and 210 km/hr were considered. Considering the above factors, this study takes cyclic load amplitudes of 80 kPa, 85 kPa, and 90 kPa, respectively.

A normalized parameter cyclic stress ratio (*CSR*) is derived by (Zhang et al. 2020), demonstrating the application of loading amplitude on a granular pile and is defined as

$$CSR = \frac{q_{cy}}{q_{us}} \tag{5.4}$$

where q_{cy} is the cyclic load amplitude, and q_{us} is the ultimate bearing capacity of an ordinary granular pile in static conditions. The ultimate bearing capacity of an OGP composed of optimum mix proportion (25% TC + 75% AG) from static loading tests is determined as 132 kPa when the loading plate is subjected to a 50 mm settlement. This study takes cyclic load amplitudes of 80 kPa, 85 kPa, and 90 kPa, corresponding to *CSR* ratios of 0.60, 0.65, and 0.70. Considering this range of *CSR* could facilitate classifying the threshold amplitude level for granular pile-reinforced soils (Ashour et al. 2022).

5.3.4.1 Behavior of granular pile under different encasements

In past studies, researchers employed either geotextile (GT) or geogrid (GG) as encasement materials. This study uses a new innovative material named combi-grid (CG), as explained in materials in Chapter 3. CG is a combination of both GT and GG. The tensile strength of the encasement material highly influences the efficacy of the vertically encased granular piles (VEGP). As the tensile strength of the encasement material increases, its influence on the granular pile improves, enhancing the overall stability of the soft soil foundation.

Fig. 5.17(a) represents the behavior of VEGPs under different encasements GT, GG, and CG, represented as geotextile encased granular pile (GTGP), geogrid encased granular pile (GGGP), and combi-grid encased granular pile (CGGP), respectively, in terms of the number of cycles (N) versus settlement (S_c), settlement reduction ratio ($S_{c,r}$), and accumulation of excess pore water pressure (P_{exc}), using the results from

test series A from Table 5.4. It can be observed that the variation of settlement versus the number of cycles for all three encasements follows the same pattern. The settlement rate is quick in the initial stages and becomes flat as the number of cycles increases. Additionally, the settlement is significantly reduced compared to OGP. It is also noticed that the settlement of GTGP is considerably higher than that of GGGP and CGGP, with the number of load cycles due to the lower tensile strength of GT compared to the other two encasement materials.

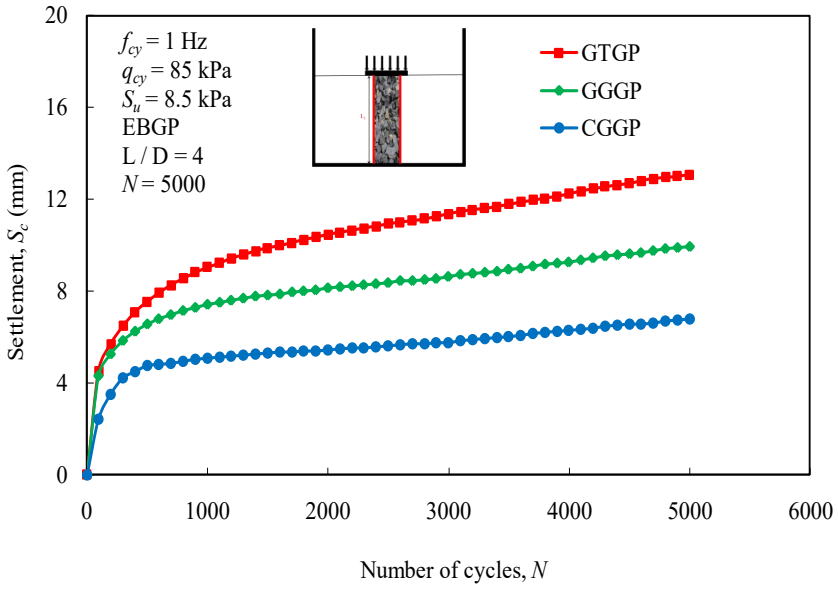

(a)

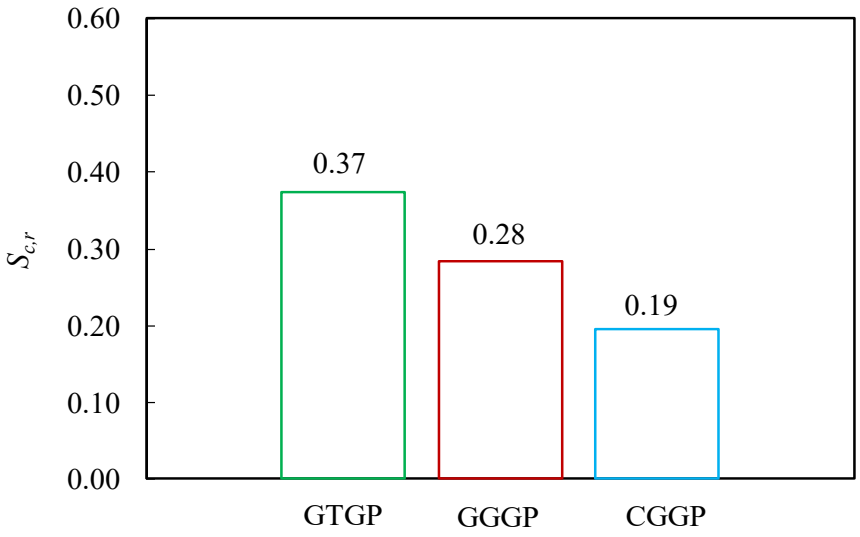

(b)

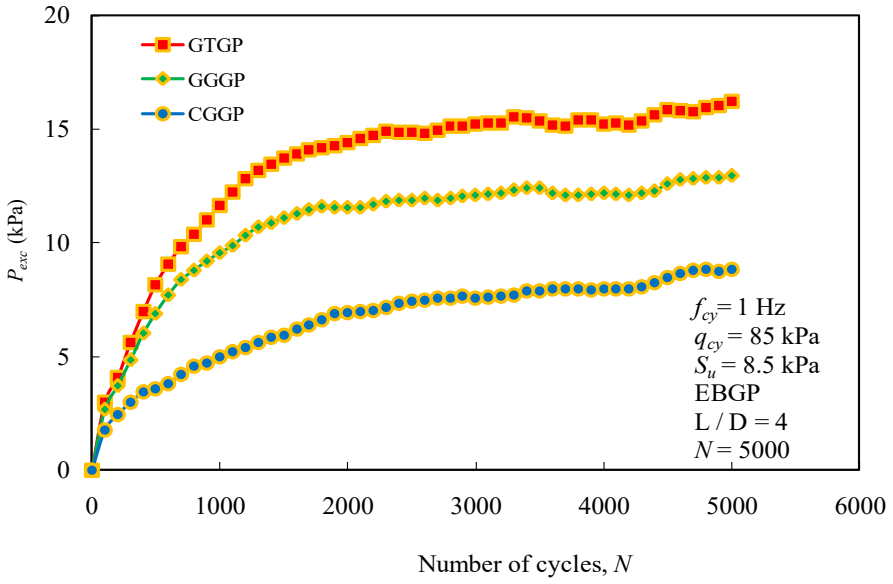

(c)

Fig. 5.17 Cyclic responses of VEGP under different encasements; (a) S_c versus N curve, (b) The settlement reduction ratio ($S_{c,r}$), and (c)P_{exc} versus N.

Fig. 5.17(b) illustrates the influence of geosynthetic encasement on the settlement reduction ratio ($S_{c,r}$), noting that a smaller $S_{c,r}$ indicates a greater reduction in cyclic-induced settlement of granular piles using the encasement material. The encasements in the form of GT, GG, and CG reduced the granular pile settlement by 63%, 72%, and 81% compared to OGP, respectively. This indicates that as the tensile strength of the encasement material increases, the $S_{c,r}$ decreases significantly. The preceding studies showed that the usage of CG is very limited in the field. However, settlement reduction is more significant with this material because it acts as both geotextile and geogrid, offering major advantages when utilized in the field. The findings highlight the significance of selecting encasement materials with the required tensile strength, not only for maximizing the performance of VEGP but also for strengthening the stability of soft soil foundations.

Fig. 5.17(c) shows the effect of encasement material on the variation of P_{exc} with the number of cycles (N), noting that granular piles with CG encasement experience

less accumulation of P_{exc} compared to GT and GG encasements. The peak P_{exc} values for CGGP, GGGP, and GTGP are 8.8 kPa, 12.9 kPa, and 16.2 kPa, respectively. One major advantage of providing geosynthetic encasements to a granular pile is their additional confinement, which stiffens the granular pile. This results in more loads being carried by the granular pile and less load being transferred to the surrounding soft soil bed.

The above results show that CG encasement is more effective at reducing P_{exc} than GT and GG encasements. The GT serves as a filter, preventing the intrusion of surrounding soft soil into the granular pile. This prevents clogging and maintains the permeability of the surrounding soil, allowing P_{exc} to dissipate more effectively because the water flow is uninterrupted by clogged soil pores, reducing the potential for water accumulation within the soil. The GG contributes to the stability and load-bearing capacity of the granular piles. It enhances the interaction between the granular piles and the surrounding soft soil, ensuring the load is transferred more effectively and efficiently. This helps prevent localized accumulation of excess pore water pressure. Combi-grid, a hybrid composite of geotextile and geogrid components, is more effective in reducing excess pore water pressure (P_{exc}) than encasements comprised solely of geotextile or geogrid. So, a vertically reinforced granular pile with combi-grid encasement (CGGP) is used in further sections.

5.3.4.2 Behavior of granular pile under different encasement configurations

The different configurations of combi-grid encasement, including full vertical length, half vertical length, horizontal encasement for full length with a spacing of 0.25D, and combined encasement for full length with a spacing of 0.25D, are presented in Fig. 5.18. These results are compared with OGP.

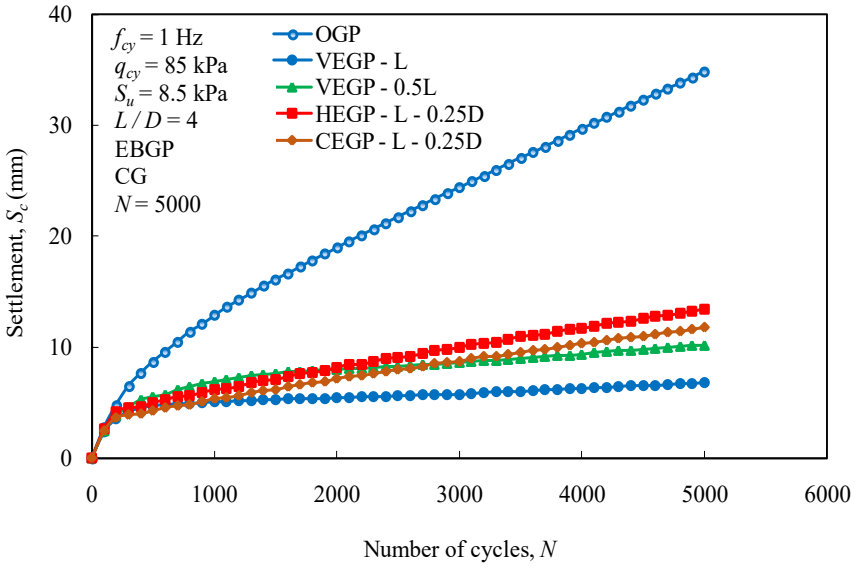

(a)

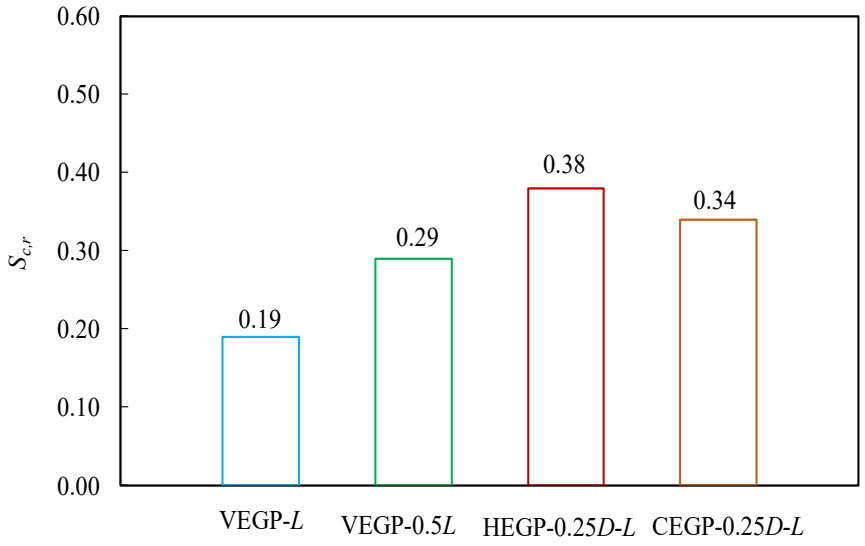

(b)

Fig. 5.18 Cyclic responses of GP under different encasement configurations; (a) S_c versus N curve, and (b) The settlement reduction ratio ($S_{c,r}$).

The gradual development of the granular pile settlement under different encasement configurations in terms of S_c versus N and $S_{c,r}$ are presented in Fig. 5.18(a). As noted, the granular pile settlement was significantly reduced when combi-grid encasement was provided in any configuration compared to OGP. S_c reduced

from 35 mm to 7 mm, 10 mm, 13 mm, and 12 mm for VEGP with full-length encasement, VEGP with half-length encasement, HEGP with a spacing of 0.25D for full length, and CEGP with a spacing of 0.25D for full length, respectively.

The relative impact of combi-grid encasement on the granular pile is also explained using the $S_{c,r}$ in Fig. 5.18(b). As noted, $S_{c,r}$ increases from 0.19 to 0.29, 0.34, and 0.38 when comparing the granular pile with full-length VEGP to half-length VEGP, CEGP with a spacing of 0.25D for full length, and HEGP with a spacing of 0.25D for full length. This indicates no significant variation in limiting granular pile settlement with different configurations. However, full-length VEGP is effective for ease of installation in the field and for preventing granular pile material intrusion into the surrounding soft soil. Considering these conditions, a combi-grid is employed as an encasement material provided as VEGP for full length and used in further studies.

5.3.4.3 Behavior of granular pile under different loading frequencies (f_{cy})

According to prior research, the effect of loading frequency (f_{cy}) is negligible or has very less effect on the soils subjected to cyclic loading (Peacock and Seed 1968; Yoshimi and Oh-Oka 1975; Wong et al. 1975; Ansal and Erken 1989; Hyde et al. 1994). However, other studies have reported that loading frequency considerably affects soils subjected to cyclic loading (Zhou and Gong 2001; Jiang et al. 2010; Yoo and Abbas 2019; Yoo and Abbas 2020). Nevertheless, the behavior of granular piles under cyclic loading frequency remains a discussion topic. This study investigates the effect of f_{cy} on the behavior of granular piles installed in soft soil using the results from test series B in Table 5.4.

Fig. 5.19 illustrates the behavior of granular piles under different loading frequencies (f_{cy} = 0.5 Hz, 1 Hz, and 2 Hz) regarding the S_c versus N, $S_{c,r,}$ and P_{exc}. It can be observed that, for OGP, at a loading frequency of 0.5 Hz, S_c decreased from 35

mm to 23 mm, and at a loading frequency of 2 Hz, S_c increased from 35 mm to 42 mm compared to the loading frequency of 1 Hz. For VEGP, at a loading frequency of 0.5 Hz, S_c decreased from 7 mm to 6 mm, and at a loading frequency of 2 Hz, S_c increased from 7 mm to 8 mm compared to a loading frequency of 1 Hz. As shown, in the cases of OGP and VEGP, S_c becomes more than 1.8 times and 1.3 times, respectively, for an increase in f_{cy} from 0.5 to 1 Hz, indicating that loading frequency is an important factor influencing the behavior of granular piles under cyclic loading. This trend is observed in Fig. 5.19(a), which represents the gradual progression of S_c with N for both OGP and VEGP cases.

The relative impact of combi-grid encasement concerning f_{cy} is explained using the $S_{c,r}$ in Fig. 5.19(b). As can be observed, $S_{c,r}$ increases from 0.16 to 0.19 when increasing f_{cy} from 0.5 to 1 Hz, and $S_{c,r}$ increases from 0.19 to 0.23 when increasing f_{cy} from 1 to 2 Hz. The results show that with the help of CG encasement, smaller cyclic loading-induced settlements, and larger cyclic loading capacities were achieved irrespective of f_{cy}. These results conclude that loading frequency (f_{cy}) significantly affects $S_{c,r}$ in the case of OGP and has very little effect in the case of VEGP.

Fig. 5.19(c) depicts the effect of cyclic loading frequency (f_{cy}) on the variation of P_{exc} for both OGP and CGGP. The accumulation of P_{exc} increases with increasing f_{cy} in both cases. The peak P_{exc} values for f_{cy} = 0.5 Hz, 1 Hz, and 2 Hz in the OGP case are 17.32 kPa, 18.98 kPa, and 20.22 kPa, and in the CGGP case are 8.60 kPa, 8.84 kPa, and 9.31 kPa, respectively. These results infer that the benefit of the CG encasement on the reduction of P_{exc} decreases as the f_{cy} increases. This observed behavior matches the settlement behavior discussed earlier.

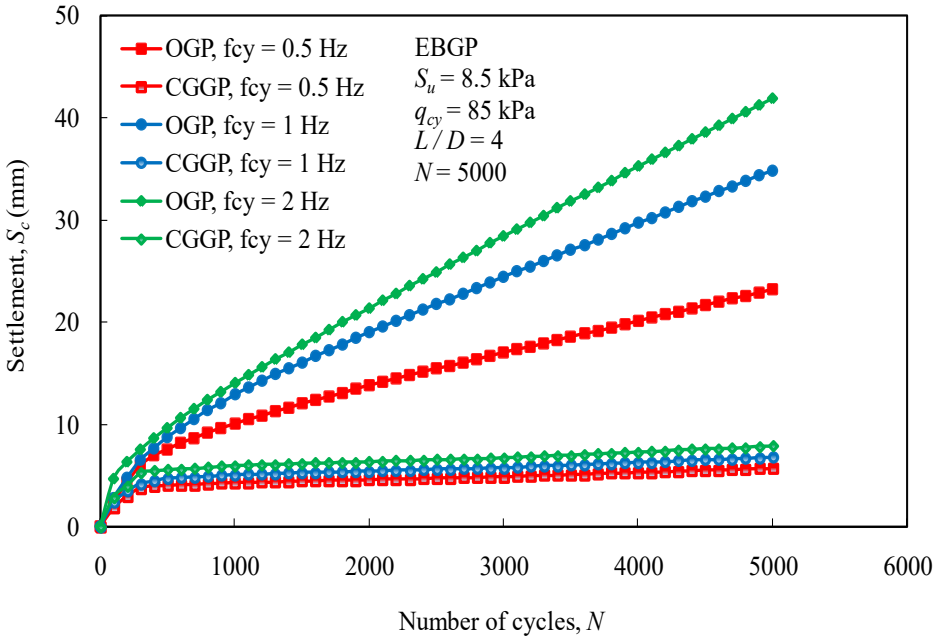
OGP, fcy = 0.5 Hz
CGGP, fcy = 0.5 Hz
OGP, fcy = 1 Hz
CGGP, fcy = 1 Hz
OGP, fcy = 2 Hz
CGGP, fcy = 2 Hz
EBGP
S_u = 8.5 kPa
q_{cy} = 85 kPa
L/D = 4
N = 5000
Settlement, S_c (mm)
Number of cycles, N
0
10
20
30
40
50
0
1000
2000
3000
4000
5000
6000

(a)

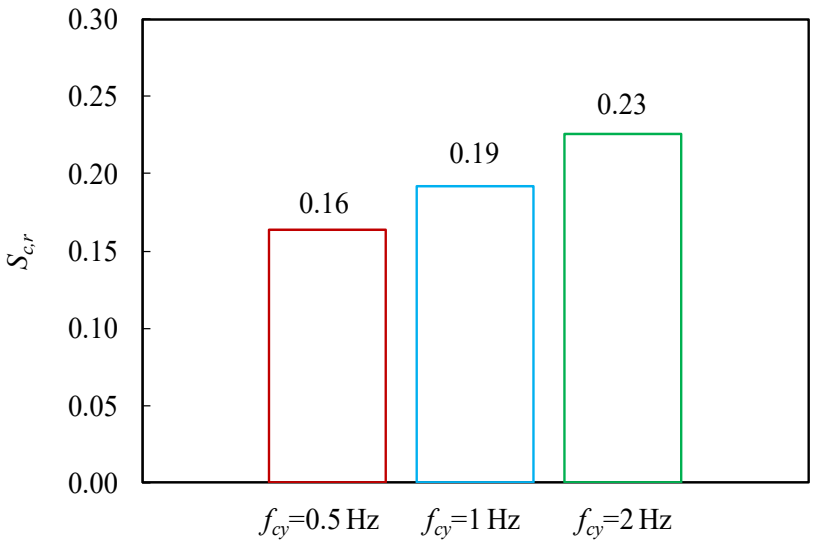
$S_{c,r}$
0.00
0.05
0.10
0.15
0.20
0.25
0.30
0.16
0.19
0.23
f_{cy}=0.5 Hz
f_{cy}=1 Hz
f_{cy}=2 Hz

(b)

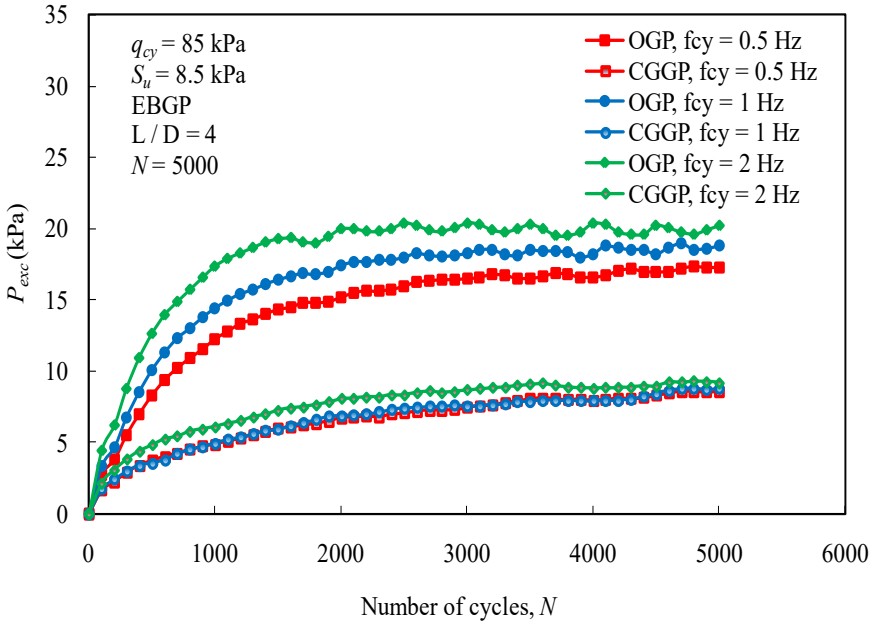

(c)

Fig. 5.19 Cyclic responses of GP under different frequencies(f_{cy}); (a) S_c versus N, (b) The settlement reduction ratio ($S_{c,r}$), and (c) P_{exc} versus N.

5.3.4.4 Behavior of granular pile under different cyclic loading amplitudes (q_{cy})

In geotechnical engineering, cyclic loading refers to the repeated application of loads or stress cycles. At lower cyclic amplitudes, the stress cycles are less severe and do not induce as much deformation in the soil and granular pile. Consequently, the potential for excessive settlement is reduced. This study examined the effect of cyclic loading amplitudes (q_{cy} = 80 kPa, 85 kPa, and 90 kPa) corresponding to *CSR* (0.6, 0.65, and 0.7), using the results from test series C from Table 5.4. The settlement behavior of granular piles under different cyclic loading amplitudes (q_{cy}= 80 kPa, 85 kPa, and 90 kPa) in terms of S_c versus N, $S_{c,r}$, and P_{exc} is presented in Fig. 5.20. As shown in Fig. 5.20(a), for OGP, S_c decreased from 35 mm to 16 mm when q_{cy} decreased from 85 kPa to 80 kPa. S_c increased from 35 mm to 50 mm within 3700 cycles before reaching 5000 cycles when q_{cy} increased from 85 kPa to 90 kPa. This indicates that limiting granular pile settlement is more effective at lower cyclic

amplitudes. Designing granular piles to limit settlement under cyclic loading is important for geotechnical structures where functionality is crucial, such as retaining walls, embankments, and infrastructure foundations. A similar trend is observed in the case of granular piles subjected to lower cyclic loading frequencies.

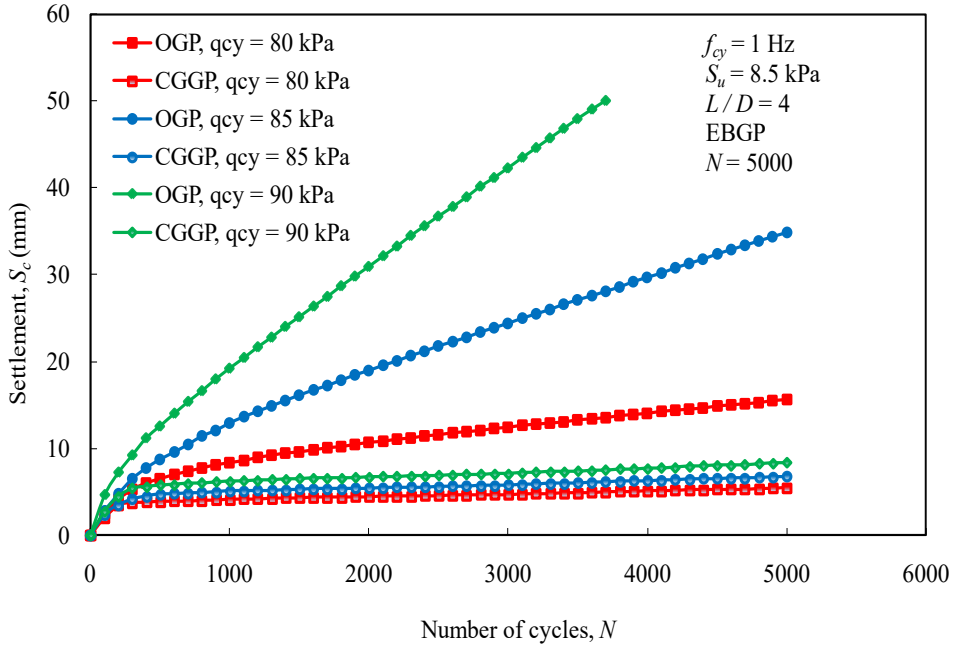

(a)

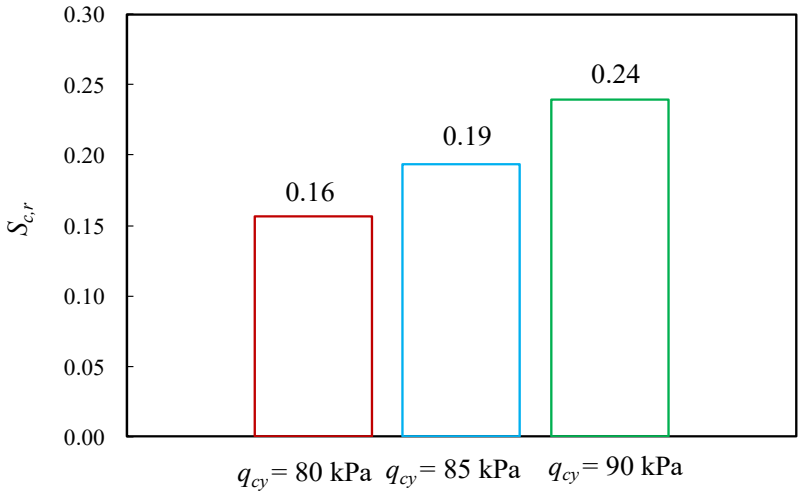

(b)

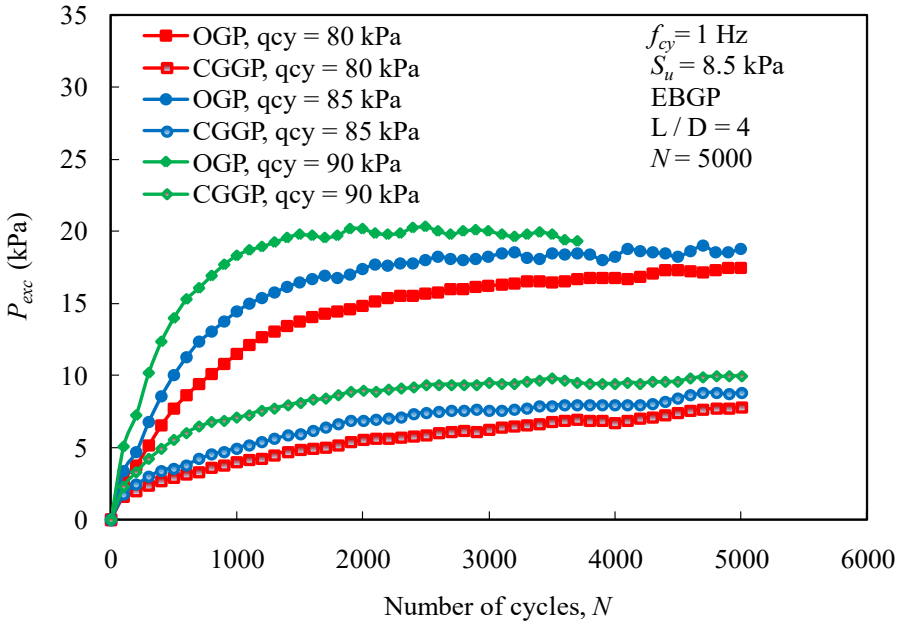

(c)

Fig. 5.20 Responses of cyclic induced settlement of GP under different cyclic amplitudes; (a) S_c versus N curve, (b) The settlement reduction ratio ($S_{c,r}$), and (c) S_c versus N curve.

The relative impact of CG encasement concerning the q_{cy} is explained using $S_{c,r}$ in Fig. 5.20(b). As noted, $S_{c,r}$ increases from 0.16 to 0.19 when q_{cy} increases from 80 kPa to 85 kPa, and $S_{c,r}$ increases from 0.19 to 0.24 when q_{cy} increases from 85 kPa to 90 kPa. The results show that with the help of CG encasement, smaller cyclic loading-induced settlements and larger cyclic loading capacities can be achieved irrespective of cyclic loading amplitudes (q_{cy}). The above results indicate that q_{cy} significantly affects $S_{c,r}$ in the case of OGP but is less effective in the case of CGGP.

The effect of cyclic loading amplitude (q_{cy}) on the variation of P_{exc} for both OGP and CGGP is presented in Fig. 5.20(c). The accumulation of P_{exc} increases with the increase in q_{cy} in both cases. The peak P_{exc} values for q_{cy} = 80 kPa, 85 kPa, and 90 kPa in the OGP case are 17.47 kPa, 18.98 kPa, and 20 kPa, respectively. In the CGGP case, the peak P_{exc} values are 7.77 kPa, 8.84 kPa, and 10 kPa, respectively. The

variation in P_{exc} for both conditions can be attributed to the load transfer mechanism: in the case of OGP, more loads are transferred to the surrounding soil bed, whereas in the case of CGGP, significantly less load is transferred to the surrounding soil bed due to the CG encasement.

5.3.4.5 Behavior of granular pile under different *L/D* ratio

Fig. 5.21(a) represents the behavior of granular piles under different *L/D* ratios (*L/D* = 4, 5, and 6) in terms of S_c versus N, $S_{c,r}$, and P_{exc}. It can be observed that, in the case of OGP, with an increase in the *L/D* from 4 to 5, S_c decreased from 35 mm to 28 mm. With an increase in the *L/D* from 4 to 6, S_c decreased from 35 mm to 23 mm. Thus, in the case of OGP, the *L/D* ratio is a key parameter, and the settlement of the granular pile reduces with an increment in the *L/D* ratio.

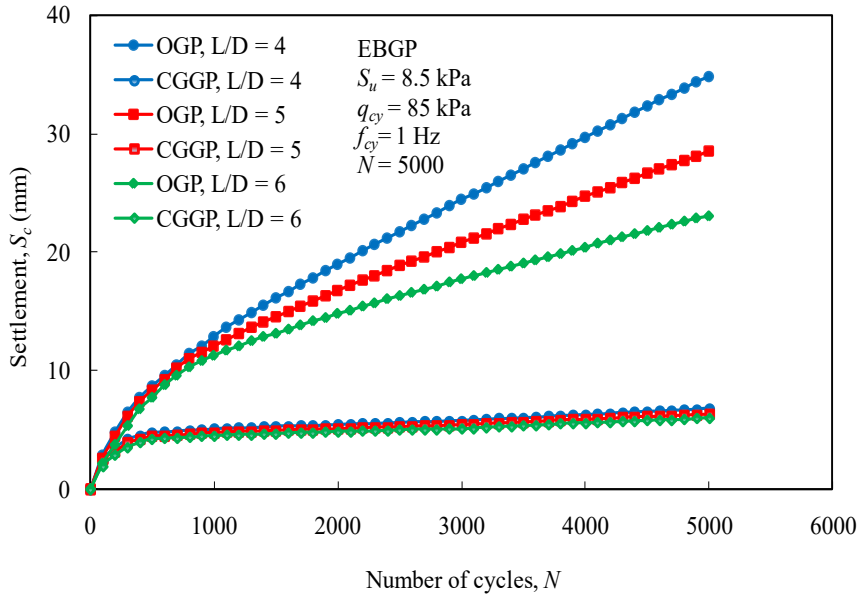

(a)

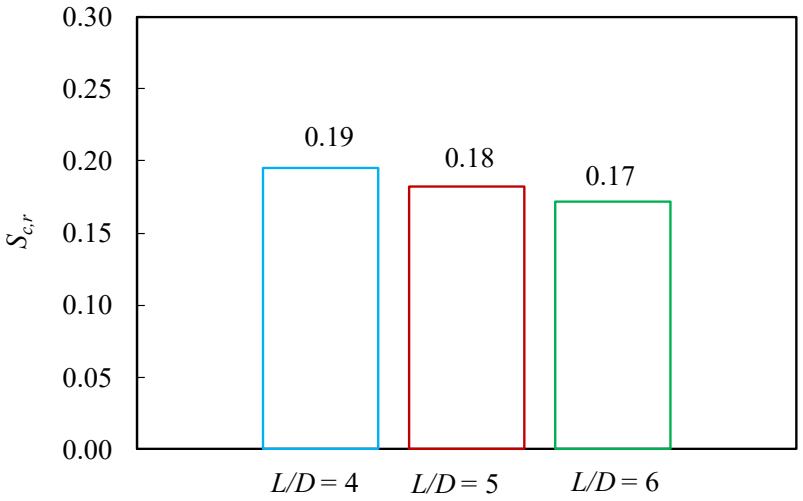

(b)

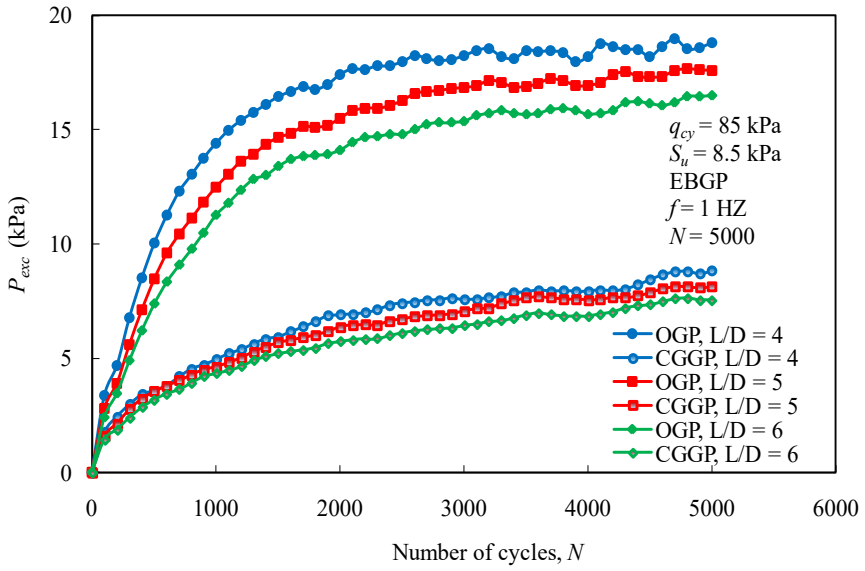

(c)

Fig. 5.21 Responses of cyclic induced settlement of GP under different *L/D*; (a) S_c versus *N* curve, (b) The settlement reduction ratio ($S_{c,r}$), and (c) P_{exc} versus *N*.

The effect of CG encasement concerning the *L/D* ratio is explained in Fig. 5.21(b) regarding $S_{c,r}$. In the case of CGGP, the settlement of the granular pile is reduced by 81%, 82%, and 83% concerning *L/D* ratios of 4, 5, and 6, respectively, compared to OGP with an *L/D* ratio of 4. It can be noted that, in the case of CGGP, there are

minimal differences in the settlement reduction concerning the *L/D* ratio. Therefore, with the provision of CG encasement, the maximum settlement reduction is achieved even at a lower *L/D* ratio, effectively reducing the length of the granular pile in the field and the project's overall cost.

The effect of the length-to-diameter ratio (*L/D*) on the variation of P_{exc} for both OGP and CGGP is presented in Fig. 5.21(c). The accumulation of P_{exc} decreases with increasing the *L/D* ratio in both cases. The peak P_{exc} values for *L/D* = 4, 5, and 6 in the OGP case are 18.98 kPa, 17.69 kPa, and 16.49 kPa, respectively, and in the CGGP case are 8.84 kPa, 8.14 kPa, and 7.62 kPa, respectively.

5.3.4.6 Behavior of granular pile under different end conditions

Fig. 5.22(a) presents the settlement response of granular piles under different end conditions (end bearing and floating) regarding S_c versus *N,* $S_{c,r,}$ and P_{exc}. Preceding studies carried out by (Ardakani et al. 2018; Shahu et al. 2023) on both end-bearing and floating granular piles reported that the end-bearing encased granular piles are very effective in reducing cyclic loading-induced settlement and offering higher resistance compared to floating encased granular piles. In this study, S_c is 35 mm, 41 mm, 7 mm and 9 mm in the cases of EB OGP, FL OGP, EB CGGP and FL CGGP, respectively.

The relative effect of the granular pile end condition is also explained using the settlement reduction ratio ($S_{c,r}$) in Fig. 5.22(b). As noted, $S_{c,r}$ is 0.19 in the case of end-bearing granular piles and 0.25 in the case of floating granular piles. It can be concluded that granular piles with an end-bearing condition are more effective than those with a floating condition.

Fig. 5.22(c) represents the effect of end bearing and floating conditions on the variation of P_{exc} with the number of cycles (*N*). It concludes that the accumulation of

P_{exc} is higher in the floating condition than in the end-bearing condition. The peak P_{exc} values for FL OGP, FL CGGP, EB OGP, and EB CGGP are 25.17 kPa, 16.14 kPa, 18.98 kPa, and 8.84 kPa, respectively. The FL OGP shows a similar pattern to EB OGP. Still, in the case of FL CGGP, the accumulation of P_{exc} is very rapid in the initial cycles and gradually decreases as the number of cycles increases.

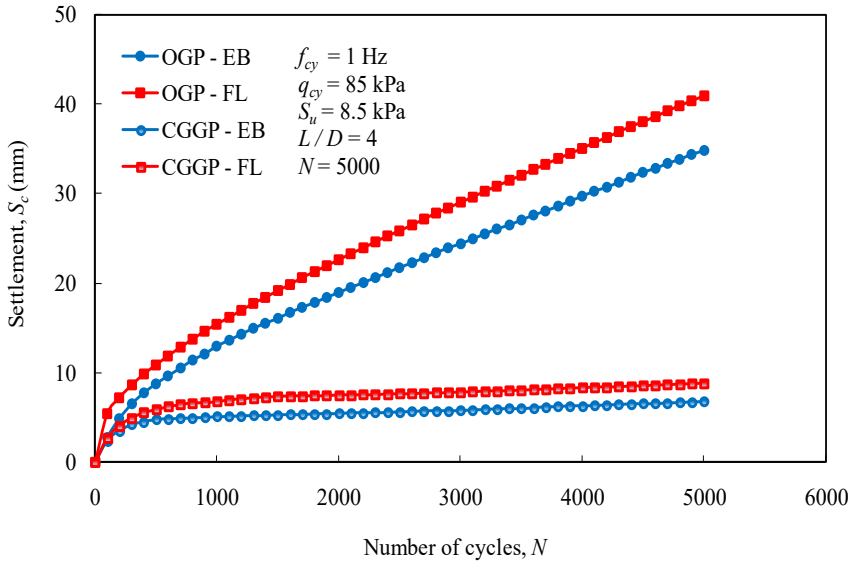

(a)

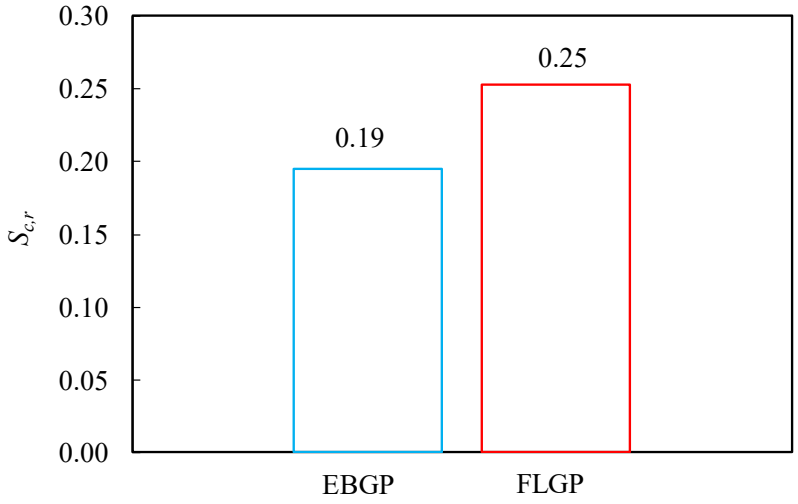

(b)

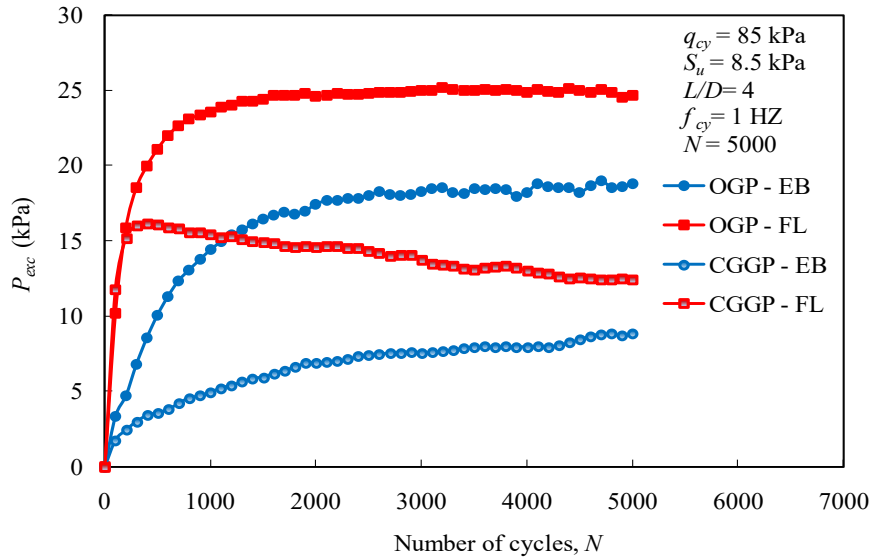

(c)

Fig. 5.22 Responses of cyclic induced settlement of GP under different end conditions; (a) S_c versus N curve, (b) The settlement reduction ratio ($S_{c,r}$), and (c) P_{exc} versus N curve.

5.3.4.7 Behavior of granular pile under different soil conditions

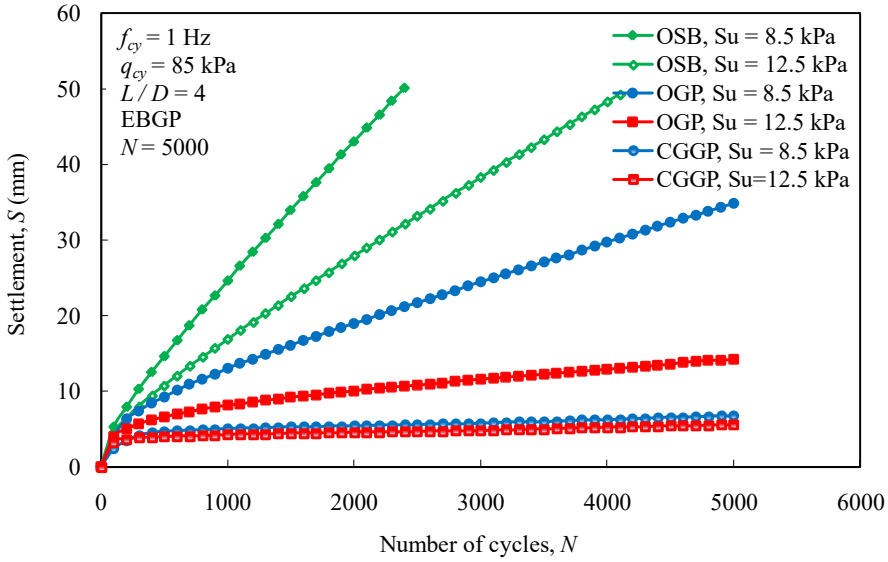

(a)

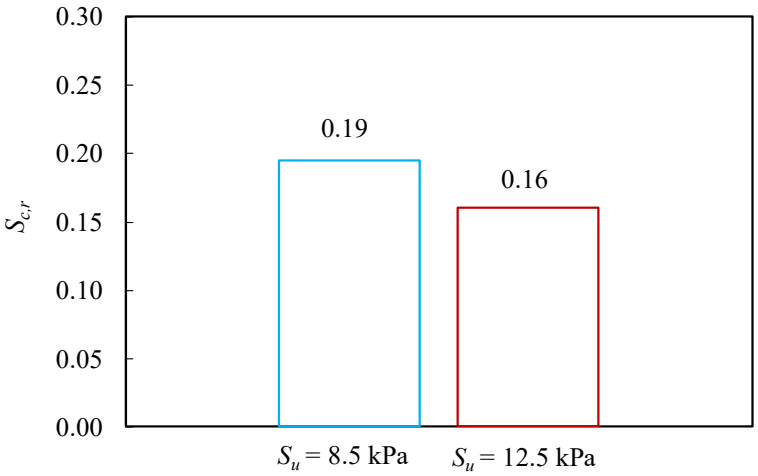

(b)

Fig. 5.23 Responses of cyclic induced settlement of GP under different soil conditions; (a) S_c versus N curve, and (b) The settlement reduction ratio ($S_{c,r}$).

The settlement response of OSB, OGP, and CGGP under different surrounding soil conditions (S_u = 8.5 kPa and 12.5 kPa) is presented in Fig. 5.23(a). Fig. 5.23 shows the gradual increase in cyclic-induced settlement (S_c) as the number of cycles (N) increases. In the case of OSB with S_u = 8.5 kPa, a 50 mm settlement is reached within 2500 cycles, while with S_u = 12.5 kPa, a 50 mm settlement is reached within 4100 cycles. For OSB in both conditions, the settlement rate increases rapidly as the N value increases.

In this study, the settlement of OGP is 35 mm and 15 mm at S_u = 8.5 kPa and12.5 kPa, respectively. Meanwhile, the settlement of CGGP is 6.8 mm and 5.60 mm at S_u = 8.5 kPa and 12.5 kPa, respectively. This suggests that the strength of surrounding soft soil significantly affects only the soil bed and OGP, exerting less influence on VEGP with CG encasement. The ultimate load-bearing capacity of OGP depends on the passive resistance and strength of the surrounding soil. The load transfer mechanism is less efficient in soft soil conditions, leading to higher stresses and settlement in granular piles. However, CGGP mitigates the impact of soft soil strength on load

distribution and settlement. The encasement enhances load-bearing capacity, stress transfer, and load distribution, enabling CGGP to perform effectively even in surrounding soft soil with varying strength characteristics. This makes them a valuable solution for ground improvement in geotechnical engineering projects.

5.4 Summary

This chapter presents the results obtained from laboratory model tests on the single granular pile in a soft soil bed under static and cyclic loading and the interpretations from the results. These results conclude that ordinary granular piles (OGP) with (0% TC + 100% AG) and (25% TC + 75% AG) maintain nearly 100% efficiency both in the case of static and cyclic loading, making a 25% tire chip content optimal for effective waste utilization without compromising load-bearing capacity (q_{us}), cyclic induced settlement (S_c) reduction, and excess pore water pressure (P_{exc}) reduction.

Using a combi-grid as a vertical encasement significantly increases the ultimate bearing capacity of granular piles with a (25% TC + 75% AG) mixture, resulting in a capacity 2.20 times greater than that of OGPs with a (0% TC + 100% AG). Additionally, the optimal configuration is a combined encased granular pile (CEGP) with a 0.25D spacing, providing a bearing capacity 1.76 times that of VEGP and 1.22 times that of horizontally encased granular piles (HEGP) with 0.25D spacing.

Similarly, the combi-grid encasement significantly reduces cyclic induced settlement (S_c) by approximately 4.50 times compared to OGP with (0% TC + 100% AG), showcasing its superior performance under cyclic loading. Additionally, the excess pore water pressure (P_{exc}) is notably reduced with granular piles. The P_{exc} values for soil bed, OGP, and VEGP with (25% TC + 75% AG) are 27.2 kPa, 18.7 kPa, and 8.9 kPa, respectively. This indicates a 31.3% reduction in P_{exc} for OGP and a remarkable 67.2% reduction for VEGP. These findings underscore combi-grid

encasement's effectiveness in improving load-bearing capacity and significantly mitigating S_c and P_{exc}, thereby enhancing the overall stability and performance of granular pile foundations in soft soil beds.

OGPs show notable effectiveness in enhancing the cyclic capacity of soft soil beds under specific conditions, particularly lower frequencies (f_{cy}), reduced cyclic amplitudes (q_{cy}), higher length-to-diameter (L/D) ratios, and end-bearing conditions. These results underscore the importance of selecting appropriate loading parameters. The application of combi-grid encasement (VEGP) improves cyclic behavior significantly, even under challenging conditions such as higher cyclic frequencies, increased amplitudes, lower L/D ratios, weaker soil conditions, and varied granular pile end conditions. Additionally, there is a significant difference in P_{exc} between OGP and VEGP, with OGP generating nearly twice the P_{exc}. These results emphasize the superior performance of combi-grid encasements in reducing S_c and P_{exc} and improving the overall stability of granular piles in soft soil beds subjected to cyclic loading.